Age, geology, geophysics, and geochemistry of Mahukona Volcano, Hawai`i

Michael O. Garcia, Diane Hanano, Ashton Flinders, Dominique Weis, Garrett Ito & Mark D. Kurz

Bulletin of Volcanology
Official Journal of the International Association of Volcanology and Chemistry of the Earth`s Interior (IAVCEI)

ISSN 0258-8900

Bull Volcanol
DOI 10.1007/s00445-012-0602-4

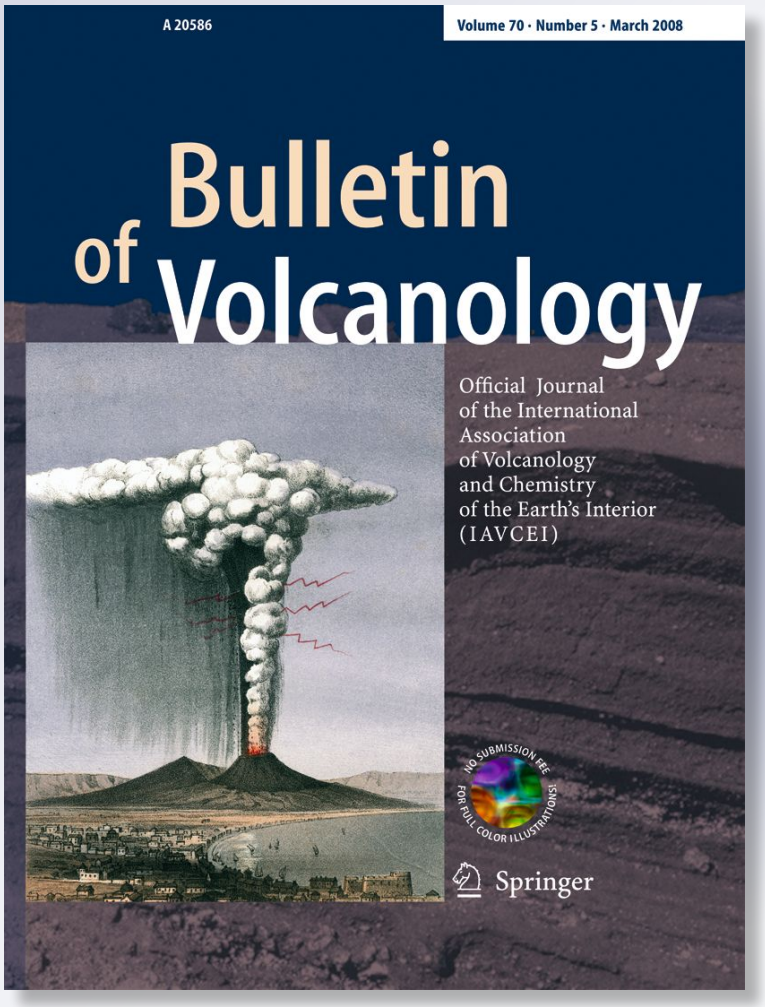

Springer

Bull Volcanol
DOI 10.1007/s00445-012-0602-4

RESEARCH ARTICLE

Age, geology, geophysics, and geochemistry of Mahukona Volcano, Hawai`i

Michael O. Garcia · Diane Hanano · Ashton Flinders · Dominique Weis · Garrett Ito · Mark D. Kurz

Received: 5 June 2011 / Accepted: 25 March 2012

Abstract The size, shape, and magmatic history of the most recently discovered shield volcano in the Hawaiian Islands, Mahukona, have been controversial. Mahukona corresponds to what was thought to be a gap in the paired sequence (Loa and Kea trends) of younger Hawaiian volcanoes (<4 Ma). Here, we present the results of marine expeditions to Mahukona where new bathymetry, sidescan sonar, gravity data, and lava samples were collected to address these controversies. Modeling of bathymetric and gravity data indicate that Mahukona is one of the smallest Hawaiian volcanoes (~6,000 km^3) and that its magmatic system was not focused in a long-lived central reservoir like most other Hawaiian volcanoes. This lack of a long-lived magmatic reservoir is reflected by the absence of a central residual gravity high and the random distribution of cones on Mahukona Volcano. Our reconstructed subsidence history for Mahukona suggests it grew to at least ~270 m below sea level but probably did not form an island. New ^{40}Ar–^{39}Ar plateau ages range from 350 to 654 ka providing temporal constraints for Mahukona's post-shield and shield stages of volcanism, which ended prematurely. Mahukona post-shield lavas have high ^{3}He/^{4}He ratios (16–21 Ra), which have not been observed in post-shield lavas from other Hawaiian volcanoes. Lava compositions range widely at Mahukona, including Pb isotopic values that straddle the boundary between Kea and Loa sequences of volcanoes. The compositional diversity of Mahukona lavas may be related to its relatively small size (less extensive melting) and the absence of a central magma reservoir where magmas would have been homogenized.

Keywords Hawai`i · Submarine volcanism · ^{40}Ar–^{39}Ar ages · Glass compositions · Mantle plume · Gravity

Editorial responsibility: MA Clynne

Electronic supplementary material The online version of this article (doi:10.1007/s00445-012-0602-4) contains supplementary material, which is available to authorized users.

M. O. Garcia (✉) · A. Flinders · G. Ito
Department of Geology-Geophysics, University of Hawai`i, Honolulu, HI 96822, USA
e-mail: mogarcia@hawaii.edu

D. Hanano · D. Weis
Pacific Centre for Isotopic and Geochemical Research, Department of Earth and Ocean Sciences, University of British Columbia, Vancouver, BC V6T 1Z4, Canada

M. D. Kurz
Department of Marine Chemistry and Geochemistry, Woods Hole Oceanographic Institution, Woods Hole, MA 02543, USA

Present Address:
A. Flinders
University of Rhode Island, Kingston, RI 02881, USA

Introduction

Mahukona, a seamount on the northwestern flank of the island of Hawai`i (Fig. 1), is the most recently discovered shield volcano in the Hawaiian Islands. This volcano fills a gap in the Loa trend, which is the western chain of the two regularly spaced sequences of shield volcanoes forming the southernmost and youngest (<4 Ma) portion on the Hawaiian-Emperor chain (Fig. 1). This gap was first noticed by Dana (1890). The presence of Mahukona Volcano, named for the nearby town on the Island of Hawai`i, was confirmed after a bathymetric survey (Moore and Campbell 1987), and lava samples were dredged and analyzed (Garcia et al. 1990). The significance of the Loa and Kea chains of

Published online: 27 May 2012

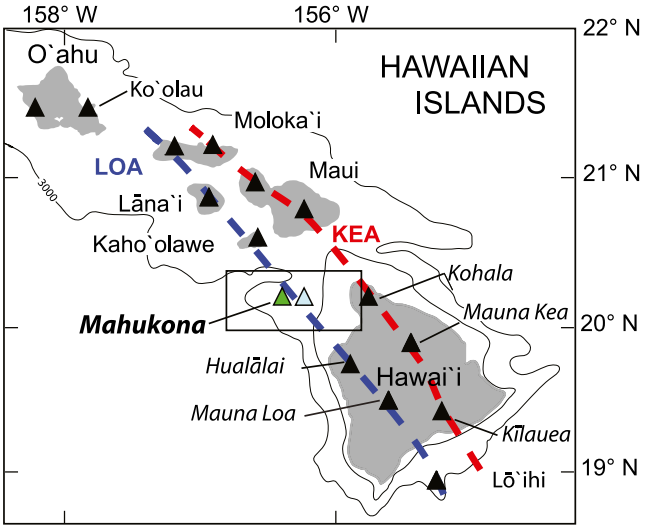

Fig. 1 Map of the Hawaiian Islands showing the Loa and Kea trends (*red* and *blue dashed lines*), location of shield volcano summit for each island (*black triangles*) with the Island of Hawai`i volcanoes identified and locations of the two proposed summits of Mahukona (*western green triangle*, Garcia et al. 1990; *eastern light blue triangle*, Clague and Moore 1991). *Box* shows location of Fig. 2, a bathymetric map of Mahukona

Hawaiian shield volcanoes has grown markedly as the lavas from the western chain (known as the Loa trend; Fig. 1) were shown to be geochemically distinct, especially for Pb isotopes, from the lavas from the eastern Kea trend (e.g., Tatsumoto 1978; Abouchami et al. 2005; Weis et al. 2011).

Previous work on Mahukona includes an overview of the geology by Garcia et al. (1990) and Clague and Moore (1991). The geochemistry of its lavas was examined by Garcia et al. (1990), Clague and Moore (1991), and Huang et al. (2009), including glass and whole-rock major, trace element, and isotope results for suites of samples collected from several areas on the volcano. These geochemical results display surprisingly large variations, greater than those shown by Mauna Kea (Huang et al. 2009), the nearby, extensively sampled giant shield volcano (e.g., Eisele et al. 2003; Stolper et al. 2004). Previous ^{40}Ar–^{39}Ar dating of lavas from two Mahukona cones yielded ages of 298±25 and 310±31 ka (Clague and Calvert 2009). No previous geophysics study has been published on Mahukona.

Here, we present new field observations, bathymetry and gravity, geochronological, petrologic, and geochemical results from three marine expeditions to Mahukona Volcano. These studies were undertaken to help resolve the questions of Mahukona's size (small vs. moderate) and summit location (buried under a carbonate platform or large cone to the west), and to better understand its volcanic structure. The new bathymetry and sidescan sonar imagery, ^{40}Ar–^{39}Ar ages, geochemical results, and gravity modeling are used to infer Mahukona's magmatic plumbing system and geologic history. The geochemical results provide new evidence for the heterogeneity of the Hawaiian mantle plume.

Geologic setting, sampling, and field observations

Mahukona Volcano is located to the west and offshore of Kohala Volcano, the oldest (last eruption ~60 ka; McDougall and Swanson 1972; Spengler and Garcia 1988) and northernmost of the five volcanoes comprising the Island of Hawai`i (Fig. 1). The size and summit location of Mahukona are debated. It has been interpreted to be relatively small (33×70×4 km, with a volume of ~3,000 km^3) and to have a summit at ~156° 25′W at a depth of ~1,080 m based on the inferred radial configuration of cones on Mahukona (Garcia et al. 1990). An alternative interpretation, based on carbonate platform slope breaks (Clague and Moore 1991), holds that Mahukona is comparable in size to nearby Hualālai Volcano (~14,000 km^3; Robinson and Eakins 2006) with a summit ~15 km to the east of 156° 25′W that is buried by coral reefs (Fig. 2). New bathymetric, sidescan sonar, and gravity surveys were carried out over Mahukona in 2009, with the R/V Kilo Moana to help resolve the size and location issues, and to better understand its volcanic structure.

Rock samples for this study were collected mainly during three Pisces V submersible dives (159, 160, and 161) on three ridges that radiate out from a large 'summit' cone at 156° 25′W and 20° 09.5′N (Figs. 2 and 3). A total of 18 lava samples (15 with glass) were collected during the 8–10-h dives covering ~2-km long traverses at water depths from 2,005 to 1,200 m. Samples (MA-xx samples) were also obtained from a dredge haul on the large summit cone (5–6 km wide, ~700 m tall, rising to 1,080 m below sea level; Fig. 2) using the R/V Atlantis II. The geochemistry for five of these samples was presented by Garcia et al. (1990). One additional glassy sample (MA-2009) was dredged during our 2009 R/V Kilo Moana surveying expedition from a cone on the southern flank of Mahukona at water depths between 2,150 and 2,435 m (Fig. 3). New ^{40}Ar–^{39}Ar ages and petrographic, glass, X-ray fluorescence (XRF), inductively coupled plasma-mass spectrometry (ICP-MS), and isotopic analyses (Pb, Sr, Nd, Hf, He) are presented here for selected samples from these expeditions. Methods used for these geochemical techniques are discussed in the Electronic supplementary material.

All of the basalts observed during our three Pisces V dives and those we dredged from Mahukona are pillow lavas indicating submarine quenching. A thin veneer (few centimeters to <1 m) of calcareous sediment drapes most pillow lavas. No volcaniclastic sediments were observed or collected during our survey of Mahukona. However, one hyaloclastite outcrop with overlying pillow lava and

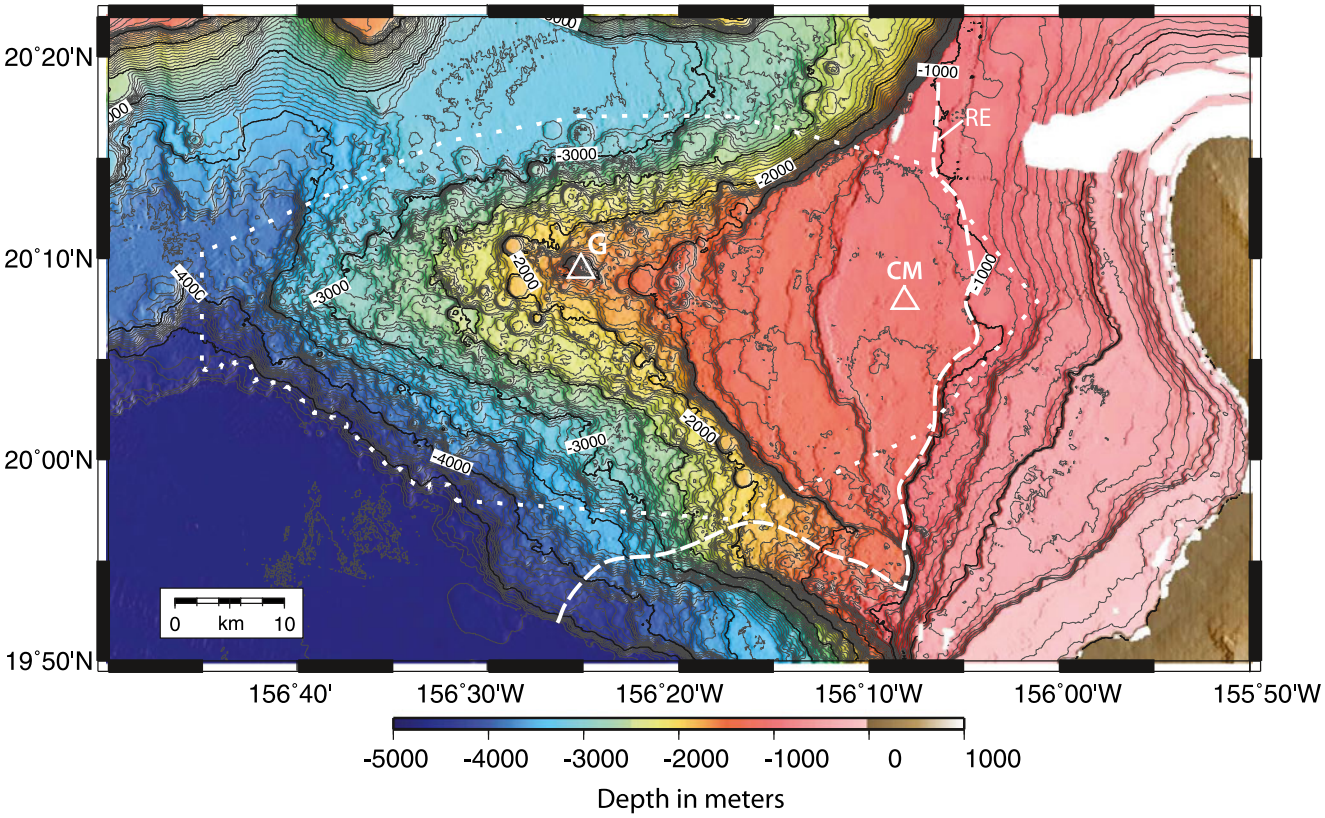

Fig. 2 Bathymetric map of the Mahukona area. Multibeam bathymetry data collected with the R/V Kilo Moana's EM120 system. The numerous circular features are flat-topped cones. *White triangles* show the Mahukona summit locations inferred by Garcia et al. (1990) "*G*" and Clague and Moore (1991) "*CM*". Contour interval is 50 m (*light thin gray lines*) with 500 m intervals shown by *heavier dark lines* with every 1,000 m contour labeled. Grid size is 75 m. This and Figs. 3 and 4 were produced using the GMT Software (Wessel and Smith 1998). Gridded data available at http://www.soest.hawaii.edu/HMRG/Multibeam/index.php. The northwestern flank of the Island of Hawai`i is shown in *brown*. *White squares* outline the area used to compute the volume of Mahukona (see text). *Longer dashed line* and labeled "*RE*" outlines the area inferred by Robinson and Eakins (2006) to be Mahukona

carbonate reef was observed on the eastern edge of Mahukona (Clague and Moore 1991). The significance of these observations is discussed below.

Bathymetry

Mahukona Volcano is an elongate bathymetric high that emerges from under a carbonate platform connecting it with neighboring Kohala Volcano (Fig. 2). The volcano's basic structure consists of one prominent central ridge projecting perpendicular to the nearby northwest coastline of the island of Hawai`i. This basic elongate structure is similar to that of the submarine volcano Lō`ihi on the south flank of the Island of Hawai`i (e.g., Fornari et al. 1988; Fig. 1). Sixty-three cones were identified in our new bathymetry and sidescan sonar images (Figs. 2 and 3). The bathymetric criterion for cone recognition was the presence of at least two closed 20 m contours, which distinguishes cones from terraces or other constructional features (e.g., Wanless et al. 2006). Mahukona cones are widely scattered across the volcano, including at its northern and southern contacts with sediment (up to 17 km off the central ridge; Figs. 2 and 3), unlike most Hawaiian volcanoes where cones occur only along rift zones and at their summit (e.g., Kīlauea and Lō`ihi; Holcomb 1987, Fornari et al. 1988).

Submarine volcanic cones are classified by their morphology; typical shapes include flat-topped, pointed, and irregular (e.g., Batiza and Vanko 1983). For Hawaiian volcanoes, cone shape was suggested to be related to stage of growth with flat-topped cones forming during the shield and rejuvenated stages, and pointed cones forming during the post-shield stage (Clague et al. 2000). Exceptions were found to this evolutionary scheme on Hawai`i's active volcanoes, Mauna Loa and Kīlauea, where pointed cones formed during the shield stage (Clague et al. 2000; Wanless et al. 2006). All three types of cones were identified on Mahukona; 70% are pointed, 21% flat-topped, and 9% irregular. A previous study had recognized flat-topped and pointed cones on Mahukona (Clague et al. 2000). Our new bathymetric and sidescan sonar maps (Figs. 2 and 3) reveal many more flat-topped cones on Mahukona than previously

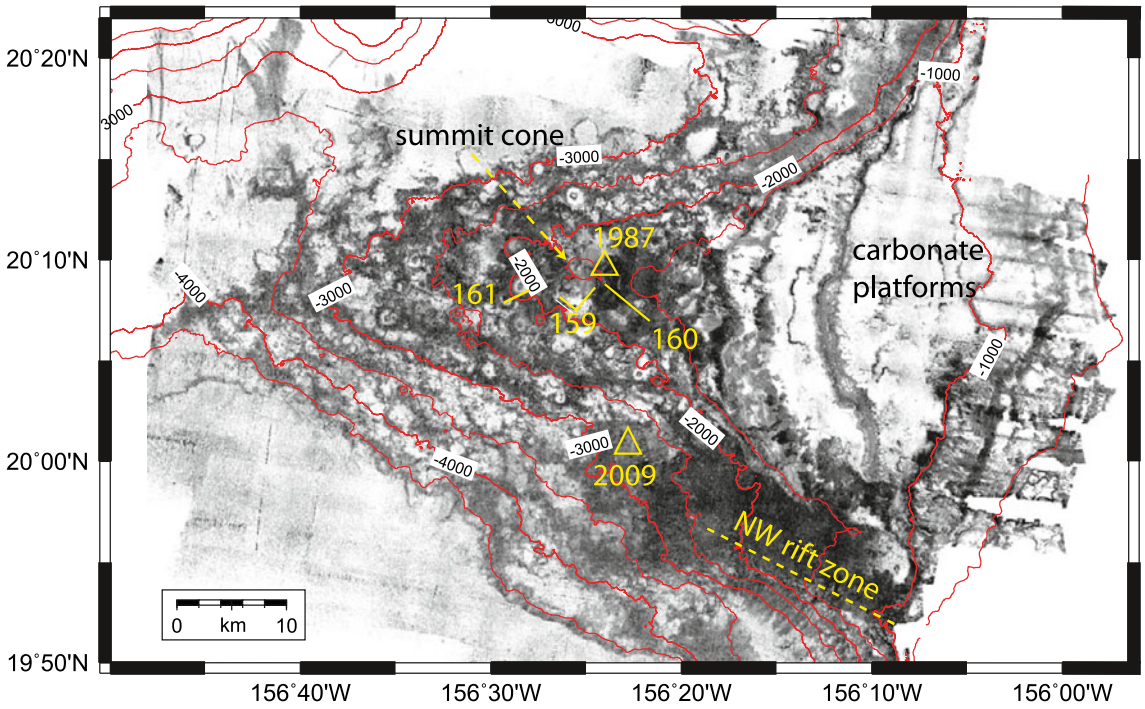

Fig. 3 Sidescan sonar map of Mahukona area. Acoustic backscatter data collected with Kilo Moana's EM120 system (50 m grid size). Strength of acoustic return increases linearly with *gray shade*. *Dark* areas indicate loud echoes, which have thin sediment and/or hard rock; *light* areas indicate soft echoes, which have thicker sediment. Sample locations for dives 159–161 (*solid yellow lines*) and dredgehauls in 1987 and 2009 (*yellow triangles*) are shown. Locations of Hualālai's northwest rift zone, Mahukona's summit cone, and the carbonate platform between Mahukona and Kohala volcanoes are also indicated on this map. *Red lines* show 500 m contour intervals with labels for every 1,000 m contour

noted, although far fewer than observed for submarine rejuvenated sequences off the northern Hawaiian Islands of Ni`ihau and Ka`ula (Garcia et al. 2008). The dominance of pointed cones was unexpected based on the abundance of tholeiitic lavas on Mahukona (e.g., Garcia et al. 1990; Clague and Moore, 1991; Huang et al. 2009) and the evolutionary scheme that was proposed by Clague et al. (2000) for Hawaiian submarine cone shape.

Most Mahukona cones are circular (75%); the others are elongate or irregular in shape. Median diameter of the pointed cones is smallest (0.9 km with standard deviation of 0.4 km); flat-topped cones are the widest (2.1 km±0.4 km), and the irregular cones are intermediate in width (1.7±0.7 km). Cone heights vary markedly: from 50 to ~700 m, with the pointed cones reflecting the extremes. The median cone height is somewhat higher for flat-topped cones (125±40 m) than for pointed cones (80±106 m) and irregular cones (88±70 m). Mahukona cones occur in a broad range of water depths (1,150–4,400 mbsl), although only pointed cones occur below 3,200 mbsl (Fig. 2). This observation contrasts with a previous one that suggested pointed cones are restricted to shallow depths due to degassing (Clague et al. 2000). This depth restriction is not valid for Mahukona or Lō`ihi Volcano, where pointed cones are also found at depths >3,000 m (Fornari et al. 1988).

The new sidescan sonar map of Mahukona shows the volcano is a mixture of highly reflective rocky (dark) and sediment covered (light) areas (Fig. 3). The dark areas include the shallow summit cone complex and the flanks of flat-topped cones. The northwest rift zone of Hualālai also is highly reflective (Fig. 3). Hualālai's rift is thought to be a younger geologic feature than Mahukona (Moore and Campbell 1987). The sidescan sonar map confirms this inference with the Hualālai rocks being darker (less sediment cover) than those from Mahukona (Fig. 3). The heavier sediment-covered areas on and around Mahukona include the abyssal ocean floor surrounding Mahukona on three sides, the tops of the flat-topped cones, and the coral reef platform on the east flank (Fig. 3). The coral platform is broken by five steps, which are acoustically reflective. These steps represent different sea-level stages increasing in age with depth from 14 to 435 ka (Moore et al. 1990; Ludwig et al. 1991).

Gravity

A marine gravity survey over the Mahukona region was made during our 2009 R/V Kilo Moana expedition. The intent of the survey was to locate and map the gravity signal

related to the volcano's high-density magma reservoir, which occurs at other Hawaiian shield volcanoes (e.g., Hualālai and Kaua`i; Kauahikaua et al. 2000; Flinders et al. 2010). To eliminate unreliable data, we manually removed high-frequency noise typically associated with changes in survey speed and direction. The internal consistency of the shipboard data (9,908 points) was improved by correcting for discrepancies in measurements at the 141 crossing points of the 25 survey lines using the crossover method of Prince and Forsyth (1984). The standard deviation of the reduced crossover errors was 0.75 milligals (mGal), which provides an estimate of the accuracy of our gravity data. Corrections for the attraction of the topography/bathymetry as well as the base of the crust, which takes the shape of a flexed elastic lithospheric plate were performed using the methods described by Flinders et al. (2010). Assumed densities were 1,000 kg/m^3 for water, 2,750 kg/m^3 for the crust below sea level, 2,300 kg/m^3 for the crust above sea level, and 3,300 kg/m^3 for the mantle. These densities and an elastic plate thickness of 30 km minimized the variation in the resulting residual gravity anomaly (RGA; Fig. 4).

Variations in the RGA reveal a density structure that deviates from that in the assumed density model. Nearly zero or negative values of RGA (green to blue in Fig. 4) overlie crust that is less dense than the reference. These values occur on the west and northern flanks, and the shallow northeast portion of Mahukona, and the northern half of the carbonate platform, including the area where Clague and Moore (1991) located the summit of Mahukona. A broad area of positive RGA (yellow to red; Fig. 4), which overlies relatively dense crust, is centered over Mahukona's southern flank. The highest RGA (20–25 mGal) is localized in an elongate (~40 by 10–15 km) area that extends NW from Hualālai's rift zone. This anomaly roughly coincides with the area of high reflectivity in the sidescan sonar map (Fig. 3), presumably where eruptions occurred most recently. This area of high RGA is also visible (albeit at much lower resolution) in the residual gravity anomaly produced from the GLORIA survey (Kauahikaua et al. 2000).

The southern portion of the high RGA zone can be interpreted as related to dense (i.e., >2,700 kg/m^3) cumulates within Hualālai's NW rift zone (Fig. 4). However, the notable northward bend and broadening of the high RGA zone complicates the interpretation of Hualālai rift zone as the only source of dense cumulates. The bathymetric expression of Hualālai's rift zone only extends to ~19°55′N, and there is no evidence in the bathymetry for it bending

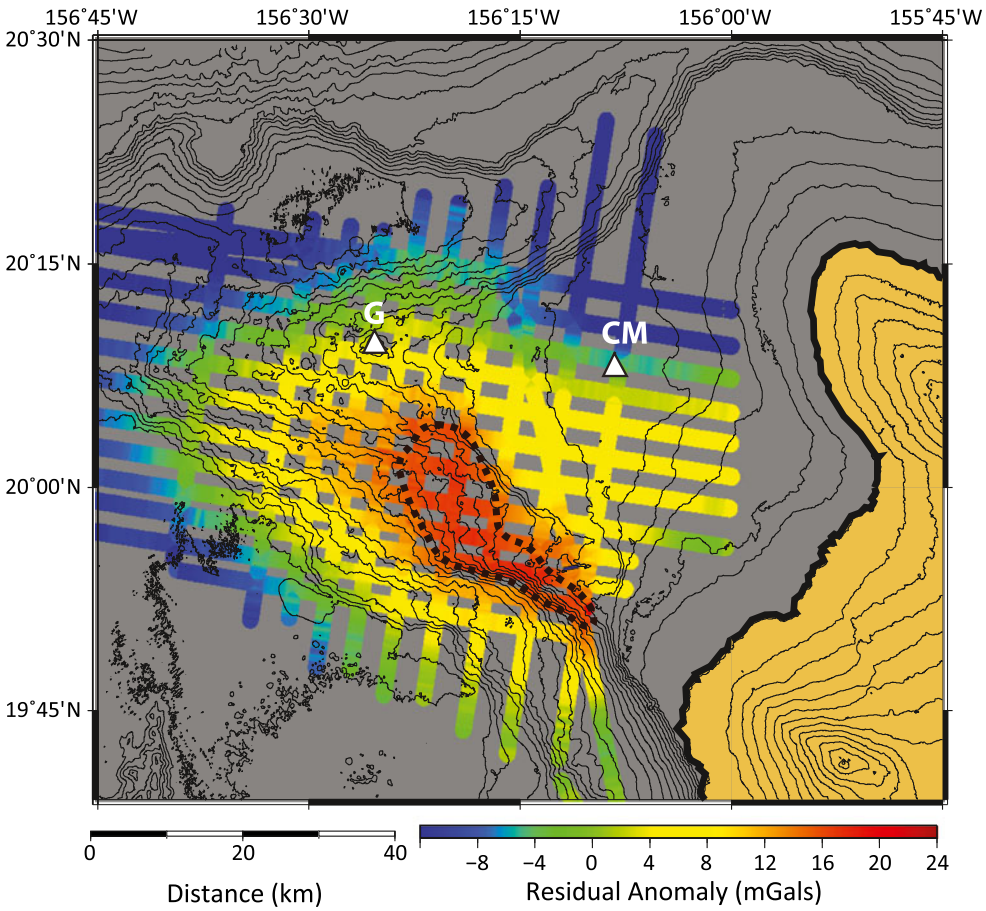

Fig. 4 Residual gravity map of the Mahukona area. Residual gravity along ship tracks are colored with superimposed bathymetry contours (200 m interval). The *dashed black line* outlines residual gravity anomaly (>±20 mGal) overlying the densest crust in the survey area. The Island of Hawai`i is shown in *gold* with shoreline shown by the *heavy black line*. The *white triangles* show the location of the proposed summits of Mahukona (*G* Garcia et al. 1990; *CM* Clague and Moore 1991)

north and following the high RGA zone. Thus, we infer that the northern portion of the high RGA zone is related to Mahukona Volcano.

Geochronology

Three Mahukona samples (one from each Pisces V dive) were selected for ^{40}Ar–^{39}Ar dating (Table 1; see the Electronic supplementary material for plateau and isochron figures and related data). These samples were chosen to span a range in depth of collection and rock composition. The plateau ages for these samples represent a high percentage of the ^{39}Ar (77%, 96%, and 96%) and have low MSWD values (0.09 and 0.13 for older ages, 0.80 for younger age; Table 1). Thus, the ages are considered to be experimentally reliable. The sample recovered in deepest water (1,970 mbsl) along the axis of the central ridge (161–2), is a tholeiite with a plateau age of 654±36 ka (1 sigma). The intermediate depth sample (159–6), collected on the south flank at 1,685 mbsl, is transitional in composition between alkalic and tholeiitic basalt and yielded a plateau age of 481±37 ka. The shallowest sample (160–5), collected from the summit cone complex at ~1,200 mbsl, is also transitional basalt and gave a plateau age of 350±16 ka. The three ages show a decreasing trend with shallower depth (Table 1).

A previous geochronology study of transitional basalt samples from two cones yielded ages of 298±25 ka (for the same cone represented by sample 160–5) and 310±31 ka for a deeper cone at 2,800 mbsl about 16 km west of the tholeiitic sample 161–2 (Clague and Calvert 2009). The previous and new ages for the shallow cone are almost within analytical error (298±25 ka vs. 350±16 ka), so we assume an age of ~325 ka for the age of the summit cone. This summit cone has high reflectivity on the sidescan sonar map (Fig. 3), so this age may represent one of the youngest periods of volcanism on Mahukona. If so, Mahukona stopped erupting well before its neighbor Kohala Volcano (last eruption 60 ka; McDougall and Swanson 1972). The ages for the Mahukona transitional basalts are considered to be indicative of its post-shield stage of volcanism because they are younger than our new age for tholeiitic basalt (Fig. 5). Kohala's younger volcanism was hawaiitic (~250–60 ka; Spengler and Garcia 1988; Fig. 5). No hawaiitic lavas have been recovered from Mahukona (see below). Thus, the shield and post-shield stages of volcanism on Mahukona were probably unusually short-lived based on the relatively small lava volumes produced during these stages compared with other Hawaiian volcanoes (e.g., Mauna Kea Volcano; Frey et al. 1990).

The 653 ka date for the tholeiitic lava is within the predicted age range for Mahukona shield volcanism (>470 ka; Moore and Campbell 1987; Garcia et al. 1990; Clague and Moore 1991). Clague and Calvert (2009) suggested tholeiitic volcanism continued until 430 ka based on a tholeiitic flow draping a dated coral reef, which is slightly younger but within analytical error of our age of 479±75 ka for a transitional lava (Table 1). Tholeiitic and transitional volcanism were coeval on Lō`ihi (Garcia et al. 2006) and Mauna Kea (Frey et al. 1990), so it is possible they were on Mahukona. Alternatively, as discussed below, this tholeiitic flow may be from Kohala Volcano. The new ages for tholeiitic and transitional volcanism on Mahukona are coeval with volcanism on Kohala and Mauna Kea volcanoes (Figs. 1 and 5).

Petrography

Thin sections were examined for 23 Mahukona lava samples. These samples are unaltered or weakly altered (thin iddingsite rims, <0.01 mm, on olivine). Olivine phenocrysts (width >0.5 mm) are present in all rocks with abundances ranging from 0.1 to 28.0 vol.% (Table 2). Deformed olivine (internal kink bands or subgrain boundaries) are present in more than half of the samples (comprising up to 100% of the phenocryst population; Table 2). Olivine xenocrysts are common in Hawaiian submarine basalts and are mainly thought to be derived from crustal cumulates from the same volcano (e.g., Clague et al. 1995; Garcia 1996). Spinel

Table 1 ^{40}Ar–^{39}Ar ages for selected Mahukona lavas

Sample	Rock type	Water depth[a] (mbsl)	^{39}Ar (%) steps	Plateau		Normal isochron			Subsidence (m) at 2.6 mm/year	Eruption depth[b] (m)
				Age±1σ (ka)	MSWD	Age±1σ (ka)	MSWD	$^{40}Ar/^{36}Ar_i$±1 σ		
160-5	Trans	1,200	76.9, 5/11	350±16	0.80	347±81	1.09	295.8±12.1	900	300
159-6	Trans	1,685	96.4, 8/10	481±37	0.09	487±63	0.10	295.0±3.3	1,245	440
161-2	Thol	1,970	95.8, 7/10	654±36	0.13	678±78	0.13	294.4±3.1	1,700	270

Thol tholeiitic, *Trans* transitional

[a] Depth of sample collection

[b] Eruption depth is subsidence rate times age, subtracted from water depth

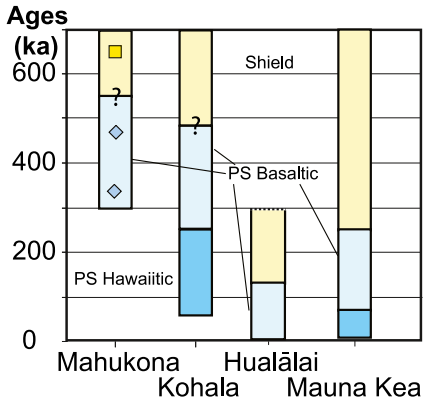

Fig. 5 Summary of the ages of shield (*yellow*) and post-shield (*blue*) stages of volcanism for Mahukona, Kohala, Hualālai, and Mauna Kea volcanoes. The new ages for Mahukona (Table 1) are shown by the *blue diamonds* (post-shield) and *yellow square* (shield). The youngest age is an average of the new and previous ages for the shallow summit cone (325 ka; see text). The post-shield stage (*PS*) is subdivided into the basaltic (*light blue*) and hawaiitic (*darker blue*) substages (Frey et al. 1990) for the Kea trend volcanoes (Mauna Kea and Kohala); the Loa trend volcanoes do not have a hawaiitic substage. Age information for Mahukona (Table 1); Kohala (Spengler and Garcia 1988); Hualālai (Sherrod et al. 2007); and Mauna Kea (Wolfe et al. 1997). *Question marks* indicate that the precise age of shield to post-shield transition is unknown

inclusions are present in many Mahukona olivines. Most samples contain euhedral to subhedral plagioclase, and many contain clinopyroxene (cpx) phenocrysts or microphenocrysts (0.1–0.5 mm across; Table 2). Samples with cpx phenocrysts lack deformed olivines (except sample 160–8 with 0.2 vol.% deformed olivine; Table 2). The presence of plagioclase and cpx in these Mahukona lavas indicates the host magmas crystallized beyond olivine control probably in a shallow magma chamber (e.g., Wright 1971), which is consistent with the glass chemistry discussed in the next section.

Glass chemistry

The new Mahukona glasses show a wide range in composition with MgO contents ranging from 5.0 to 7.8 wt.% and K_2O varying from 0.40 to 0.68 wt.%, which is wider than previously reported (Fig. 6; Table 3). The glasses can be subdivided into two basic geochemical groups: tholeiitic and transitional (Fig. 6). The new tholeiitic samples were all collected from deeper depths (>1,950 mbsl) and can be subdivided into two distinct SiO_2 subgroups (< and >52 wt.% SiO_2). The lower

Table 2 Modes for Mahukona lavas based on 500 point counts/sample

Sample	MgO (wt.%)		Olivine			Plagiolcase		Clinopyroxene		Spinel	Matrix
	rock	glass	phen	deformed	mph	phen	mph	phen	mph	mph	
159-1	22.55	7.80	10.4	17.6	4.0	–	–	–	–	<0.1	68.0
159-4	11.11	6.27	4.8	3.2	7.2	–	5.6	–	<0.1	–	79.2
159-5	10.44	6.35	1.6	–	14.2	–	7.0	–	–	–	77.2
159-6	9.21	6.32	1.6	–	10.6	–	7.4	–	–	–	80.4
160-1	10.01	6.45	1.2	0.6	10.2	–	1.6	–	–	–	86.4
160-2	8.65	5.05	4.4	–	6.4	–	6.6	3.4	5.6	–	73.6
160-3	nd	5.43	2.4	–	5.6	5.8	12.0	2.8	4.0	–	67.4
160-4	9.77	5.49	2.2	–	5.8	3.6	9.6	0.8	5.8	–	72.2
160-5	8.83	nd	2.8	2.4	6.4	2.8	6.4	–	–	–	79.2
160-6	8.56	nd	3.2	–	3.6	6.4	6.0	1.2	7.2	–	72.4
160-7	9.85	nd	1.0	–	2.0	4.4	6.2	1.6	5.0	–	79.8
160-8	8.92	5.54	1.2	0.4	3.6	1.0	6.2	0.8	3.4	–	80.4
161-1	17.64	5.99	7.6	12.6	7.2	–	–	–	–	–	72.6
161-2	16.29	6.10	12.0	4.6	3.6	0.8	1.2	–	–	–	77.8
161-3	14.04	5.50	11.2	11.0	5.0	–	5.2	–	–	–	67.6
161-4	20.19	7.53	12.6	11.2	6.6	0.4	2.4	–	–	–	66.8
161-5	9.30	6.17	–	1.4	5.4	–	–	–	–	–	93.2
161-6	11.54	6.38	1.6	1.8	4.8	–	0.3	–	–	–	88.8
MA-1	nd	6.50	–	–	0.1	–	0.3	–	–	–	99.6
MA-3	8.09	nd	1.1	–	–	–	0.3	–	<0.1	–	98.6
MA-12	9.36	nd	0.7	–	–	–	0.2	–	<0.1	–	99.0
MA-21	nd	6.25	–	–	0.1	–	–	–	–	–	99.9
MA-32	11.27	6.71	–	–	0.1	–	–	–	–	–	99.9

Mineral abundances are reported vesicle-free in volume percent

Crystal sizes: *phen* (phenocryst, >0.5 mm); *mph* (microphenocrysts, 0.1–0.5 mm; *MA* sample modes from Garcia et al. (1990); *nd* not determined

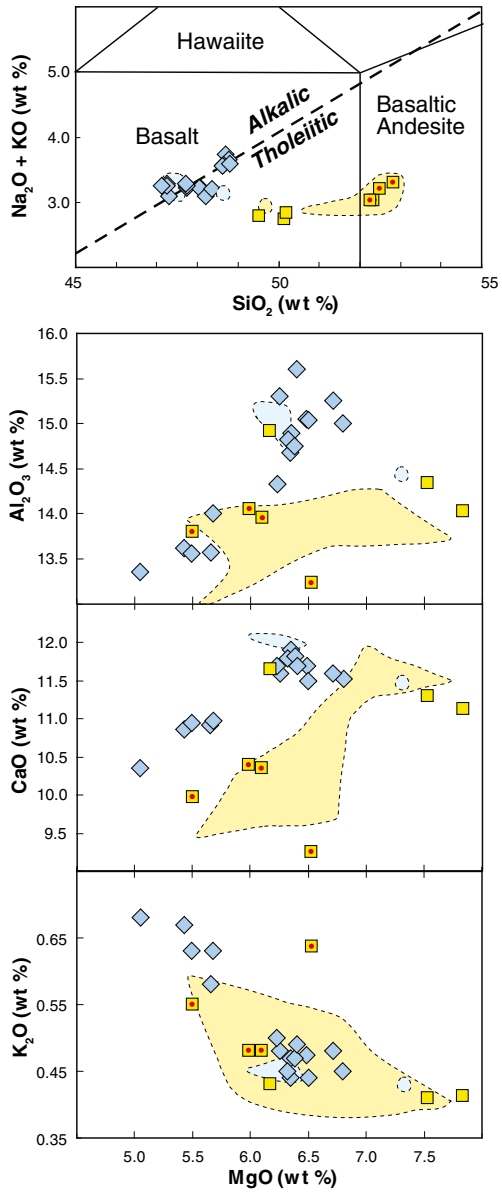

Fig. 6 MgO variation diagrams and total alkalis vs. SiO_2 plot of glass chemistry for Mahukona samples. *Symbols* for new data (Table 3): *yellow squares*, tholeiites (*solid red dot* added for higher SiO_2 samples, >52 wt.%); *blue diamonds*, transitional basalts (compositions along or near the alkalic–tholeiitic dividing line. Fields for previous data (Clague and Moore 1991; Clague and Calvert 2009) are *yellow* for tholeiitic samples and *light blue* for transitional glasses. *Upper plot* is total alkalis vs. SiO_2 with alkalic–tholeiitic *dashed dividing line* from Macdonald and Katsura (1964) and classification grid from Le Bas et al. (1986). *Lower plots* are MgO variation diagrams for selected major elements. The decrease in Al_2O_3 and CaO with decreasing MgO contents indicates crystallization of plagioclase and clinopyroxene, respectively. Note the overlap in K_2O contents for many tholeiitic and transitional samples with the same MgO value

SiO_2 samples also have lower TiO_2 and K_2O contents (Fig. 6) and are similar to the Group B tholeiites of Huang et al. (2009). Compared with the Group B tholeiites, the new lower SiO_2 samples have somewhat higher Al_2O_3 contents but otherwise substantially overlap with those previously reported (Fig. 6). The new transitional glasses also form two clusters; the cluster with higher total alkalis has lower MgO (<5.7 wt.%) indicating that these glasses are more fractionated (Fig. 6; Table 3). Fractionated glasses were not previously reported from Mahukona (Fig. 6). These fractionated samples are the only Mahukona lavas with common (>4 vol.%) cpx crystals (Table 2). The transitional glasses form relatively coherent trends on MgO variation diagrams suggesting similar parental magma composition (Fig. 6). The glass chemistry shows decreasing CaO and Al_2O_3 vs. decreasing MgO below 6.5 wt.% MgO indicating crystallization of plagioclase and cpx (Fig. 6), which is consistent with the presence of phenocrysts of these minerals in most of the rocks (Table 2). Sulfur contents of the new Mahukona glasses range from 0.038 to 0.088 wt.%, indicating that these lavas underwent variable amounts of degassing in shallow to moderate water depths (<500 m to >1 km; e.g., Moore and Fabbi 1971).

Whole-rock major and trace element chemistry

MgO contents of the new Mahukona lavas range widely with the tholeiites generally having higher MgO concentrations than the transitional rocks (9.1–22.5 vs. 8.1–11.3 wt.%; Table 4) similar to previously reported results (Fig. 7). The only major differences in whole-rock composition between new and previous data are the higher K_2O content of the new tholeiites and the wider range of the new transitional samples (Fig. 7). The K_2O of transitional samples varies somewhat at the same MgO content, suggesting multiple distinct parental magmas. In contrast, all but one of the tholeiitic samples form a simple linear MgO variation trend (Fig. 7). The distinct sample is similar to group B of Huang et al. (2009). The new and previous CaO and Al_2O_3 data show good linear trends with no inflection for each rock group on MgO diagrams (Fig. 7), indicating that cpx and plagioclase crystals were not removed from or added to the host magma and that olivine was the primary fractionating mineral. The absence of plagioclase fractionation interpretation is supported by the good correlation of Sr with highly incompatible elements (Table 4). None of the new or previously reported Mahukona rocks have hawaiitic compositions (Fig. 5), which are typically produced during the late post-shield stage on Kea trend volcanoes (e.g., Kohala, Mauna Kea, Haleakalā, West Maui; Macdonald et al. 1983; Spengler and Garcia 1988; West et al. 1988). Hawaiites have not been found on neighboring Loa-trend volcano Hualālai either (e.g., Moore et al. 1987). Several samples contain slightly higher MnO contents (<0.20 vs. 0.26–0.34; Table 4), which may be related to minor amounts of MnO contamination from the surface coating on these samples.

Table 3 Microprobe analyses of Mahukona glasses

Sample	Depth	Type	SiO_2	TiO_2	$Al2O_3$	FeO	MnO	MgO	CaO	Na_2O	K_2O	P_2O_5	S	Total
159-1	1,975	Thol	49.52	2.32	14.03	11.15	0.17	7.83	11.14	2.37	0.41	0.21	0.081	99.23
159-4	1,875	Trans	47.73	2.84	14.68	12.03	0.19	6.35	11.83	2.74	0.47	0.26	0.080	99.20
159-5	1,805	Trans	48.08	2.84	14.89	11.66	0.18	6.35	11.91	2.78	0.44	0.24	0.055	99.37
159-6	1,685	Trans	48.05	2.81	14.82	11.81	0.18	6.32	11.79	2.77	0.45	0.24	0.088	99.24
160-1	1,515	Trans	47.25	2.93	15.04	12.15	0.18	6.48	11.70	2.81	0.47	0.26	0.055	99.33
160-2	1,415	Trans	48.70	3.60	13.35	14.20	0.19	5.05	10.35	3.05	0.68	0.33	0.036	99.50
160-3	1,250	Trans	48.78	3.32	13.62	13.14	0.19	5.43	10.86	2.99	0.67	0.32	nd	99.28
160-4	1,200	Trans	48.64	3.43	13.55	13.40	0.19	5.49	10.95	2.94	0.63	0.30	nd	99.52
160-8	1,220	Trans	48.63	3.35	13.56	13.47	0.23	5.65	10.92	2.97	0.58	0.35	0.038	99.76
161-1	2,005	Thol	52.35	2.81	14.05	10.16	0.14	5.99	10.40	2.55	0.48	0.29	0.065	99.18
161-2	1,970	Thol	52.25	2.80	13.95	10.15	0.16	6.10	10.35	2.55	0.48	0.28	0.038	99.07
161-3	1,940	Thol	52.50	2.96	13.80	10.57	0.16	5.50	9.97	2.65	0.55	0.31	0.046	98.97
161-4	1,970	Thol	50.15	2.20	14.34	10.63	0.16	7.53	11.30	2.33	0.41	0.21	0.043	99.26
161-5	1,960	Thol	50.05	2.37	14.92	11.06	0.17	6.13	11.81	2.44	0.44	0.23	nd	99.62
161-6	1,930	Trans	48.20	2.70	14.75	11.50	0.17	6.38	11.82	2.62	0.47	0.25	0.046	98.86
MA-1[a]	dred	Trans	47.30	2.80	15.04	11.97	0.18	6.50	11.50	2.65	0.44	0.34	nd	98.72
MA-15	dred	Trans	47.74	2.76	15.60	11.67	0.17	6.40	11.70	2.76	0.49	0.34	nd	99.63
MA-21[a]	dred	Trans	47.72	2.83	15.30	11.86	0.19	6.25	11.59	2.81	0.48	0.34	0.038	99.75
MA-25	dred	Trans	48.35	2.95	14.32	12.02	0.17	6.23	11.69	2.71	0.50	0.36	nd	99.30
MA-26	dred	Trans	48.79	3.30	14.00	12.82	0.19	5.68	10.98	2.96	0.63	0.36	nd	99.71
MA-30	dred	Trans	47.25	2.77	15.00	11.78	0.18	6.80	11.53	2.81	0.45	0.34	nd	98.91
MA-32[a]	dred	Trans	47.12	2.76	15.25	11.87	0.19	6.71	11.60	2.78	0.48	0.34	0.051	99.15
MA-2009	dred	Thol	52.82	2.77	13.23	11.03	0.17	6.53	9.26	2.67	0.64	0.39	0.073	100.41

Depths in meters below sea level; oxide and *S* values in weight percent with total iron as FeO

dred dredgehaul, *nd* not determined

[a] Analysis from Garcia et al. (1990)

The XRF determined concentrations of compatible trace elements Ni and Cr generally correlate with MgO, with higher amounts for the olivine-rich tholeiites (up to 1,163 and 1,434 ppm, respectively; Table 4). Ratios of Zr/Nb, a potential source indicator, are not correlated with rock type (Table 4). The transitional and the lower SiO_2 tholeiitic lavas have Zr/Nb ratios <12, typical of Kea-type volcanoes (Rhodes et al. 1989), whereas the higher SiO_2 tholeiites have distinctly higher Zr/Nb ratios (13.5–14.0; Table 4), which are typical of Mauna Loa lavas (e.g., Rhodes and Vollinger 2004). No samples with high Zr/Nb were previously reported from Mahukona.

Incompatible elements were determined on matrix material from selected Mahukona lavas (Table 5). The mantle-normalized patterns in these samples are typical of Hawaiian basalts: limited range for the heavy rare earth element (REEs) and Y, increasing variation with degree of incompatibility and negative anomalies for Th, U, Rb, and Ba (Fig. 8). The narrow range of heavy REE (Table 5) in Hawaiian basalts is thought to be related to residual garnet in the source (e.g., Frey et al. 1990), whereas the relative depletion in the most highly incompatible elements (Rb, Ba, Th, and U) is suggestive of a prior melting event (Hofmann 1988), as noted by Huang et al. (2009). One surprising feature for the Mahukona lavas is the relatively high concentration of incompatible elements in the two higher silica lavas compared with the other tholeiitic (e.g., 30–40% higher Nb) and the transitional lavas (average 15% higher Nb; Fig. 8).

Radiogenic isotopes

The new Mahukona basalts form three groups in plots of Pb, Sr, Nd, and Hf isotopes (Fig. 9). The tholeiites separate into two groups with the higher silica samples from dive 161 having lower $^{87}Sr/^{86}Sr$ and $^{208}Pb/^{204}Pb$ ratios and higher $^{143}Nd/^{144}Nd$ and $^{176}Hf/^{177}Hf$ than the lower silica tholeiites (Figs. 9 and 10; Table 6). The transitional basalts comprise the third group, defining a coherent linear trend extending to more radiogenic Pb compositions with intermediate Sr and relatively low Hf isotope ratios compared with lavas from adjacent volcanoes (Figs. 9 and 10; Table 6). The new Mahukona

Table 4 XRF majors and trace data for Mahukona lavas

Sample	Type	SiO_2	TiO_2	Al_2O_3	Fe_2O_3	MnO	MgO	CaO	Na_2O	K_2O	P_2O_5	Total	LOI	Nb	Ba	Rb	Sr	Zr	Y	Zn	Ni	Cr	V
159-1	Thol	45.82	1.39	8.75	12.51	0.19	22.55	6.91	1.08	0.267	0.150	99.62	−0.34	7.1	59	3.9	200	83	15.6	107	1,163	1,434	168
159-4	Trans	46.67	2.39	13.47	12.77	0.18	11.11	10.37	2.13	0.456	0.240	99.79	0.27	12.4	92	5.9	329	139	25.3	126	386	592	266
159-5	Trans	46.39	2.44	13.49	13.29	0.20	10.44	10.72	2.06	0.467	0.244	99.74	0.21	12.9	90	5.8	326	140	26.3	129	322	439	286
159-6	Trans	47.13	2.65	14.13	12.45	0.18	9.21	11.33	2.19	0.461	0.254	99.98	0.17	14.0	103	5.8	341	153	28.2	128	269	392	296
160-1	Trans	46.21	2.61	13.73	13.70	0.19	10.01	10.57	2.41	0.475	0.262	100.16	0.22	13.5	98	6.4	342	152	27.5	131	311	330	284
160-2	Trans	47.59	2.52	14.15	12.58	0.19	8.65	11.09	2.34	0.486	0.266	99.86	0.26	13.5	100	7.3	331	150	28.7	127	244	406	296
160-4	Trans	47.04	2.52	13.53	13.51	0.19	9.77	10.14	2.19	0.514	0.269	99.67	1.21	13.2	85	6.1	314	155	29.1	123	232	381	268
160-5	Trans	47.54	2.49	14.24	13.00	0.19	8.83	10.85	2.08	0.448	0.277	99.95	−0.16	13.5	101	6.1	325	152	28.6	125	217	364	297
160-6	Trans	47.59	2.49	14.32	12.94	0.20	8.56	10.97	2.35	0.450	0.274	100.14	−0.02	13.6	101	6.4	327	151	29.2	125	194	329	293
160-7	Trans	46.66	2.50	13.48	13.86	0.29	9.85	10.29	2.10	0.450	0.278	99.76	1.22	13.3	97	6.0	303	156	29.0	129	255	463	280
160-8	Trans	47.48	2.51	14.04	13.07	0.20	8.92	10.85	2.23	0.455	0.261	100.02	0.02	13.4	103	6.8	321	151	28.9	128	202	327	298
161-1	Thol	47.96	2.00	9.74	12.60	0.19	17.64	7.26	1.67	0.356	0.236	99.65	−0.19	10.5	79	5.4	212	143	24.7	117	852	1,087	221
161-2	Thol	48.35	2.11	10.29	12.50	0.18	16.29	7.72	1.78	0.402	0.244	99.86	0.05	10.8	81	5.7	227	151	26.3	116	732	1,023	239
161-3	Thol	48.89	2.34	10.84	12.57	0.19	14.04	8.02	1.94	0.467	0.280	99.58	0.04	12.6	91	6.6	244	174	29.7	120	591	848	256
161-4	Thol	46.36	1.53	9.69	12.55	0.19	20.19	7.60	1.33	0.312	0.164	99.92	−0.09	7.9	73	4.3	222	91	17.1	109	947	1,121	194
161-5	Thol	48.81	2.18	13.38	12.54	0.34	9.30	10.62	1.89	0.384	0.227	99.67	0.22	11.2	99	5.5	304	134	24.0	121	270	1,114	279
161-6	Trans	46.11	2.29	12.97	13.32	0.20	11.54	10.28	2.07	0.475	0.231	99.49	0.17	12.3	89	6.0	307	134	25.3	127	362	499	272
MA-3	Trans	47.90	2.56	14.53	12.03	0.17	8.09	11.44	2.42	0.584	0.256	99.98	0.45	13.3	99	9.3	345	149	27.8	122	228	389	293
MA-12	Trans	47.62	2.53	13.96	11.95	0.17	9.36	11.05	2.37	0.570	0.256	99.84	0.45	13.5	106	9.2	349	148	27.8	130	311	463	287
MA-32	Trans	45.90	2.45	13.48	13.26	0.19	11.27	10.15	2.19	0.433	0.245	99.57	0.11	12.8	95	6.1	337	144	25.6	131	410	368	268
MA-2009	Thol	51.06	2.49	12.09	12.46	0.26	9.15	8.76	2.49	0.560	0.351	99.67	−0.20	16.1	122	8.6	283	226	35.8	121	257	504	255

Oxide values in weight percent with total iron as Fe_2O_3; trace elements in parts per million (ppm)

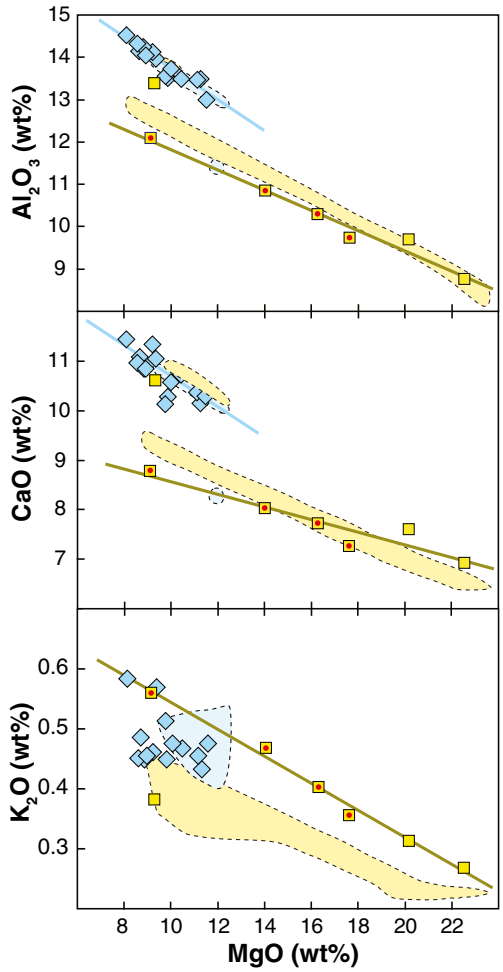

Fig. 7 MgO variation diagrams for Mahukona whole rocks (Table 4). Fields for previous data (Clague and Moore, 1991; Huang et al. 2009) are *yellow* for tholeiitic samples and *light blue* for transitional lavas. The linear trends for the tholeiitic (except one sample, 161–5) lavas indicate the whole-rock compositions were affected only by olivine fractionation and/or accumulation and were derived from parental magmas with similar major element compositions. The absence of decreasing trends for CaO and Al_2O_3, as seen in MgO plots for glass compositions (Fig. 6), indicate that the samples have not undergone fractionation of pyroxene or plagioclase. *Symbols* as in Fig. 6

basalt isotope ratios generally overlap the Pb isotopic compositions of Loa trend lavas, except for two higher silica tholeiitic samples which overlap in isotopic composition with Kohala samples and have Pb isotopic compositions typifying Kea trend volcanoes in Pb–Pb space (Fig. 9). Most of the previously studied Mahukona tholeiites also have Kea-like Pb isotope values (Huang et al. 2009), although their high CaO lavas have low Pb isotope values like Kaho`olawe lavas (Fig. 9). The other new and previously studied Mahukona basalts have Loa-like Pb isotope values. Overall, the isotopic data for Mahukona tholeiitic lavas has a mixed parentage with both Kea and Loa trend compositions (Fig. 10).

New and previous isotopic data for Mahukona transitional basalts (from the post-shield stage based on their younger

Table 5 ICP-MS data for selected Mahukona matrix material

Sample	Rb	Ba	Th	U	Nb	La	Ce	Pr	Nd	Hf	Sm	Eu	Gd	Tb	Dy	Y	Ho	Er	Tm	Yb	Lu	Zr	Ta	Pb	Sc	Sr
159-1	5.71	88.6	0.65	0.21	11.1	9.58	24.3	3.45	16.1	3.25	4.47	1.58	4.88	0.75	4.50	24.6	0.88	2.33	0.34	1.86	0.27	127	0.63	1.07	–	–
159-4	5.87	82.4	0.74	0.23	12.6	10.3	25.9	3.83	17.7	3.50	4.78	1.68	5.16	0.81	4.79	26.4	0.91	2.44	0.35	1.98	0.28	138	0.71	0.72	–	–
159-6	6.40	89.4	0.80	0.26	13.8	11.4	28.1	4.11	19.0	3.76	5.21	1.83	5.65	0.89	5.28	28.7	1.01	2.62	0.38	2.22	0.32	146	0.82	0.92	–	–
160-1	6.23	88.8	0.81	0.26	13.4	11.7	27.5	4.06	19.0	3.90	5.28	1.85	5.79	0.89	5.24	28.1	0.99	2.63	0.37	2.19	0.31	147	0.78	1.02	–	–
160-2	7.19	93.8	0.71	0.25	13.4	12.2	29.8	4.41	20.6	3.82	5.62	1.90	6.17	0.97	5.55	29.6	1.06	2.76	0.39	2.33	0.35	145	0.81	1.10	31.5	339
160-5	6.64	93.8	0.67	0.29	12.7	11.6	28.3	4.20	19.6	3.65	5.37	1.80	5.82	0.92	5.37	28.5	1.02	2.64	0.37	2.26	0.34	138	0.77	1.02	31.9	326
160-6	7.17	93.8	0.71	0.30	13.5	12.4	30.0	4.45	20.7	3.85	5.69	1.91	6.19	0.98	5.62	30.4	1.08	2.81	0.39	2.42	0.37	146	0.81	1.07	31.3	334
161-2	7.63	96.7	0.83	0.30	14.6	12.5	32.2	4.86	23.0	4.87	6.42	2.22	7.12	1.10	6.47	35.7	1.21	3.28	0.47	2.64	0.38	194	0.81	3.02	–	–
161-3	8.32	107	0.99	0.35	15.8	14.4	36.0	5.41	25.9	5.58	7.27	2.44	7.85	1.22	7.13	38.8	1.36	3.61	0.51	2.97	0.41	216	0.90	1.13	–	–
161-4	6.30	87.9	0.63	0.21	11.3	9.93	23.6	3.48	16.4	3.28	4.60	1.62	5.12	0.77	4.56	25.7	0.88	2.34	0.33	1.91	0.28	130	0.64	1.05	–	–
161-6	6.63	90.8	0.77	0.26	14.1	10.9	27.7	4.07	19.2	3.89	5.25	1.85	5.75	0.89	5.41	29.8	1.03	2.74	0.40	2.28	0.32	150	0.81	0.88	–	–
MA-12	7.70	93.8	0.67	0.34	13.0	11.6	28.3	4.19	19.6	3.61	5.34	1.82	5.85	0.92	5.26	28.6	1.01	2.60	0.36	2.23	0.33	139	0.78	1.04	32.7	428
MA-32	6.14	93.8	0.68	0.21	12.8	11.5	28.0	4.15	19.4	3.62	5.30	1.81	5.73	0.90	5.12	27.2	0.96	2.49	0.35	2.12	0.32	139	0.77	1.01	30.2	345

All values are in ppm

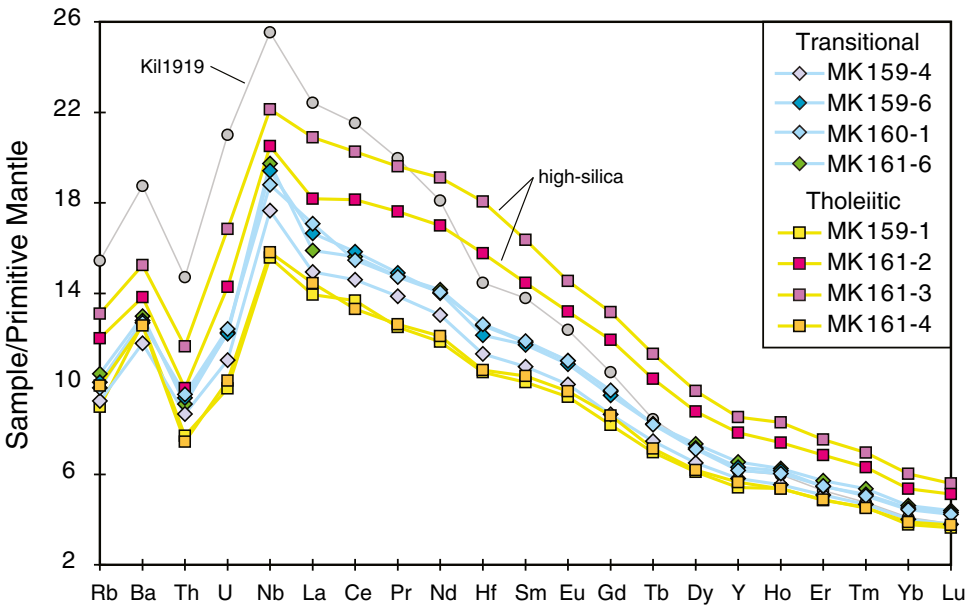

Fig. 8 Primitive Mantle normalized plot of incompatible trace elements (ICP-MS; Table 5) for Mahukona matrix material. Transitional samples are shown by *blue connecting lines*; tholeiitic lavas by *yellow lines*. Note the higher abundance of incompatible elements in the higher silica tholeiites than in all transitional lavas. Values for a reference sample, Kīlauea tholeiitic basalt (Kil1919; Pietruszka and Garcia 1999) are shown for comparison. Data normalized to primitive mantle values of McDonough and Sun (1995)

ages; Fig. 5) extend to more radiogenic Pb compositions ($^{206}Pb/^{204}Pb=18.38$; $^{208}Pb/^{204}Pb=38.14$) than the tholeiites and plot within the Lō`ihi field (Fig. 9). The apparent temporal variation towards higher radiogenic Pb isotopes matches the temporal variation for Kohala Volcano and is opposite to the trends for Hualālai and Mauna Kea volcanoes, as was noted by Hanano et al. (2010). The Sr and Hf isotopic ratios for the transitional basalts are intermediate among Hawaiian lavas and are somewhat different than the ratios for lavas from Lō`ihi (Fig. 9). These results suggest that the source for Mahukona transitional lavas is distinct from the source for the post-shield lavas from neighboring volcanoes or reflects different mixing proportions of source components (Figs. 9 and 10).

Helium isotopes

Most Mahukona glasses had extremely low helium contents (i.e., less than 10^{-8} cc STP/gram by crushing) and are assumed to be extensively degassed and unreliable for mantle helium measurements. This interpretation is consistent with the moderate eruption depths (<1,000 mbsl) inferred from the glass S contents and the low-to-moderate vesicularity of the lavas. This was confirmed by comparing He abundance and isotopic composition of glass and olivine pairs from several samples. For example, crushing of sample 161–1 glass yielded 3.0×10^{-9} cc STP/gram He, with a $^{3}He/^{4}He$ of 7.9±0.2 times atmospheric Ra, whereas olivines yielded 1.66×10^{-8} cc STP/gram He with a $^{3}He/^{4}He$ of 19.1±0.2 Ra. Due to the extremely low helium contents in the glasses, it was necessary to analyze olivine crystals by crushing, except sample MA-32 which had relatively high He concentrations in the glass (>5×10^{-7} cc STP/gram). Some Mahukona samples contain both phenocrysts and xenocrysts. Therefore, the reported olivine helium isotopic data are from a population of crystals and may not represent a single mantle source. Previous studies of Hawaiian phenocrysts show that helium co-varies with other isotopes (e.g., Kurz and Kammer 1991; Kurz et al. 2004), suggesting that the phenocrysts do represent the mantle source, which is assumed in this discussion. The helium isotope values reported here (Table 6) are a combination of new values for ten samples from dives 159–161 and two previously reported dredged samples (Garcia et al. 1990).

Overall, the new measurements (Table 6) display a similar range in $^{3}He/^{4}He$ to those previously reported (11.5-20.8 vs. 12.8-21.0 Ra; Garcia et al. 1990). The highest $^{3}He/^{4}He$ values (>20 Ra) are found in the transitional samples. These values overlap with the He isotope data from pre-shield stage alkalic and tholeiitic samples from Lō`ihi Volcano, and shield stage tholeiites from Mauna Loa and Mauna Kea volcanoes (Fig. 11). Three of the four Mahukona tholeiitic samples have lower $^{3}He/^{4}He$ values (11.5−13.7 Ra); the exception (161–1) has a value of 19.1 (Table 6). The new helium data show similar trends observed with the other radiogenic isotopes with the transitional basalts overlapping the Lō`ihi field and the tholeiites showing larger variability (Fig. 11). The isotopic overlap with the Lō`ihi field was previously used as an argument that the Mahukona lavas were produced in a shield building stage (Garcia et al. 1990). The new age data for transitional Mahukona lavas show this interpretation was incorrect. The Mahukona data do not show an anti-correlation between $^{3}He/^{4}He$ and SiO_2 content as observed at Mauna Kea (Kurz et al. 2004), although the lower SiO_2 lavas from both volcanoes have high $^{3}He/^{4}He$ values.

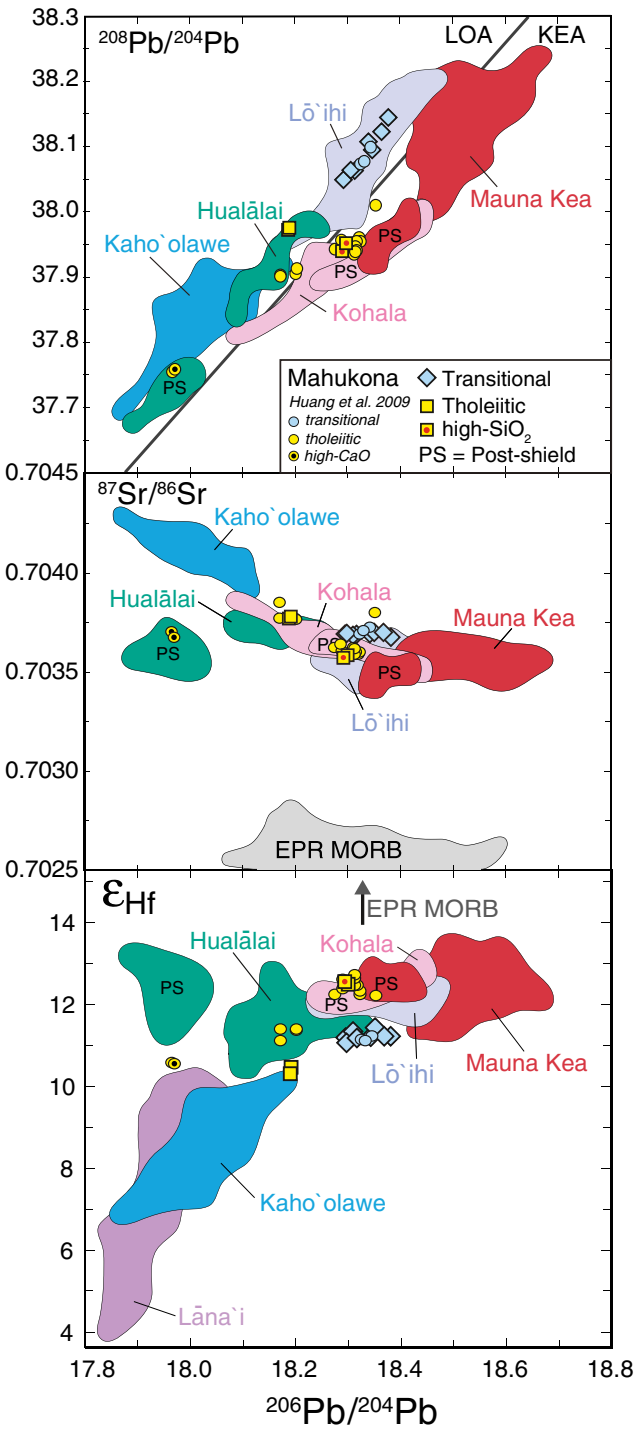

Fig. 9 $^{208}Pb/^{204}Pb$, $^{87}Sr/^{86}Sr$, and ε_{Hf} vs. $^{206}Pb/^{204}Pb$ for Mahukona lavas compared with shield and post-shield (*PS*) lavas from selected Hawaiian volcanoes. *Symbols* size is larger than 2σ error bars. Also plotted are previous data for Mahukona lavas (Huang et al. 2009), which are shown by *circles* (*yellow* for tholeiites and *blue* for transitional lavas). In the Pb–Pb plot, the *black line* represents the Loa-Kea Pb isotopic division as defined by Abouchami et al. (2005). Data sources: Lō`ihi, Blichert-Toft et al. (1999), Abouchami et al. (2005); Hualālai, Yamasaki et al. (2009), Hanano et al. (2010) Kaho`olawe, Blichert-Toft et al. (1999), Abouchami et al. (2005), Huang et al. (2005); Lana`i, Abouchami et al. (2005), Gaffney et al. (2005); Mauna Kea, Blichert-Toft et al. (2003), Eisele et al. (2003), Bryce et al. (2005), Hanano et al. (2010); Kohala, Feigenson et al. (1983), Abouchami et al. (2005), Hanano et al. (2010), D. Weis, unpublished data; EPR MORB, Niu et al. (1999), Regelous et al. (1999), Castillo et al. (2000)

Discussion

Size and structure of Mahukona

It is challenging to rigorously determine the volume of Hawaiian volcanoes. Adjacent shield volcanoes overlap in space and in the time of growth (e.g., Mauna Loa and Mauna Kea have overlapped for at least 0.5 Myrs). In addition, a correction for subsidence must be made for the portion of the volcano that has displaced the Cretaceous oceanic lithosphere (e.g., Moore 1987). Thus, it is necessary to make assumptions about the shape and the amount of subsidence for each volcano to obtain a reasonable volume estimate (e.g., Robinson and Eakins 2006).

Here, we estimated the volume of Mahukona using new bathymetric data and assuming the bathymetry is compensated by a flexed lithospheric plate. The densities used were those that minimized the RGA (Fig. 4). The range of effective elastic plate thicknesses considered (25–35 km) includes the value that minimized the RGA (30 km) as well as other estimates for the Hawaiian volcanoes (see Flinders et al. (2010) and references therein). The geographic border used for the volume estimates is shown in Fig. 2. This border is defined on the southwest based on the flat and deepest abyssal seafloor shown in Fig. 2, on the south based on the interpreted offshore extension of the Hualālai rift zone, and on the north based on the relatively flat, well-sedimented seafloor between Mahukona and Maui. Without any constraints on the extent of the eastern flank (now covered by a carbonate platform; Fig. 3), we assumed an approximately symmetrical shape for Mahukona. To negate the volume of the preexisting oceanic crust, we use the depth of the seafloor SW of Mahukona as the reference depth of the surface of the preexisting seafloor on which the volcano grew. From this depth, the surface slopes downward beneath Mahukona, taking the shape of the flexed lithospheric plate and defines Mahukona's base.

The resulting total volume of Mahukona is estimated at ~6,000 km^3, assuming an elastic plate thickness of 30 km. With no plate flexure, the volume is ~4,300 km^3 for the bathymetry shallower than 4,600 m. These volume estimates are considerably smaller than a previous estimate that assumed the summit of Mahukona is buried under the carbonate platform (13,500 km^3; Robinson and Eakins 2006). How do we tell which of these estimates is more likely to be correct?

Modeling of the new gravity data offers an independent method for assessing the size and structure of Mahukona.

Volcanoes in Hawai`i and elsewhere commonly show pronounced gravity highs over their summits, which mark their dense magmatic cores, with amplitudes that increase with volcano volume (e.g., Kinoshita et al. 1963; Clouard et al. 2000; Flinders et al. 2010). One surprising result from our gravity survey is the location of the positive RGA on Mahukona's southern flank, 10–20 km south of its bathymetric axis (Fig. 4). Although atypical and not understood, such a displacement of the highest gravity anomaly relative to the topographic summit is seen in two other Hawaiian volcanoes (Kaua`i, Flinders et al. 2010; and Hualālai, Kauahikaua et al. 2000). Another important finding is that the RGA high has low amplitude (maximum of 20–25 mGal). This is ~2–4 times smaller than the RGA of moderate size (14 to 25×10^3 km^3) Hawaiian shield volcanoes (e.g., 50 to 105 mGal; Hualālai and Ni`ihau; Kauahikaua et al. 2000; Flinders et al. 2010) and comparable to the small gravity high over Lō`ihi Volcano, which is only ~1,900 km^3 (Robinson and Eakins 2006). The small size of Mahukona's gravity anomaly suggests the volcano's volume is smaller than previously estimated (13,500 km^3; Robinson and Eakins 2006). The RGA for Mahukona is comparable to the smaller volcanoes of French Polynesia (Raivavae, Tahaa, Moorea, Mururoa), which have estimated volumes between 2,160 and 4,500 km^3 (Clouard et al. 2000). Thus, we infer Mahukona is among the smallest Hawaiian volcanoes (e.g., next smallest volcano within the Hawaiian Islands is Ka`ula at 9,600 km^3; Robinson and Eakins 2006). The gravity results do not resolve the question of the where Mahukona's magmatic center was, but suggest the center is unlikely to be under the carbonate platform (as suggested by Clague and Moore 1991) based on the low-amplitude residual gravity in that area (Fig. 4).

Why does Mahukona lack a central gravity high? Perhaps it is related to the lack of a central magmatic plumbing system. This may also be the cause of the broad distribution of cones on Mahukona, which is atypical for Hawaiian shield volcanoes. Cones on most Hawaiian volcanoes are restricted in location to the summit area and along rift zones (Macdonald et al. 1983). The exceptions include neighboring Mauna Loa and Mauna Kea volcanoes (Fig. 1). Mauna Loa cones are found not only at the summit and along its two rift zones but also randomly distributed on its west and northwest flanks (Wanless et al. 2006). These other cones are called radial vents because some of them are elongate, pointing towards the volcano's summit (Lockwood and Lipman 1987). The mechanism of formation of the Mauna Loa radial vent cones is not understood (e.g., Walker 1990; Rubin 1990). Mauna Kea cones are randomly distributed, and in contrast to Mauna Loa, most of the cones erupted evolved alkalic compositions (hawaiite and mugearite) during the volcano's late post-shield stage (West et al. 1988; Wolfe et al. 1997). These magmas are thought to have been stored at greater depths than magmas during the shield stage (~15 vs. 2–6 km) reflecting a drastically diminished magma supply (Frey et al. 1990). None of the recovered Mahukona samples have evolved alkalic compositions. Furthermore, among the ten Mahukona cones sampled in our study, seven have tholeiitic lavas and three cones have transitional compositions. Similarly, all but two of the cones sampled by Clague and Moore (1991) and Huang et al. (2009) are tholeiitic. Thus, the random distribution of cones on Mahukona does not reflect the post-shield stage of volcanism. Instead, we interpret the broad distribution of cones to be derived from both shield and post-shield stages of volcanism, and the lack of a central gravity high on Mahukona, to be related to the absence of a large central magma reservoir.

Subsidence estimate

The magnitude of Mahukona's subsidence can be inferred from the new ages, the subsidence rate for the Island of Hawai`i, and the S content of the pillow rim glasses. All Hawaiian volcanoes undergo subsidence during and after their growth (Moore 1987; Moore et al. 1990). The Island of Hawai`i is subsiding ~2.6 mm/years based on ages from carbonate terraces on the east flank of Mahukona (Ludwig et al. 1991). Using the same subsidence rate for Mahukona and assuming it has remained constant, the new ages (Table 1) suggest subsidence of ~900 m at the young, shallow summit cone, ~1,250 m at the intermediate age sample site, and ~1,700 m at the older, deeper tholeiite site. For comparison, Kohala Volcano has subsided at least 1,100 m based on the depth of a submerged shoreline terrace (which marks the end of peak volcano growth during the shield stage; Holcomb et al. 2000). Subtracting the Mahukona subsidence values from the sample collection depths suggests that these sites were submarine at the time of eruption (~270–440 mbsl). These depth estimates are consistent with the field observations that all of the lavas collected west of the summit cone are pillow lavas. However, these estimates do not negate the possibility that the lavas were erupted subaerially, flowed into the ocean, and quenched as pillow lavas (similar to lavas from the ongoing Kīlauea eruption; e.g., Mattox and Mangan 1997).

The sulfur content of Hawaiian submarine glasses is useful for inferring whether pillow lavas were erupted subaerially (e.g., Moore and Fabbi 1971; Davis et al. 2003). The moderate S contents of the new Mahukona glasses discussed here (0.03–0.09 wt.%) suggest that these lavas were not erupted subaerially. Instead, the S contents are consistent with the subsidence-adjusted depths and with the moderately vesicular character of the lavas (20–30 vol.%). Glasses collected from Mahukona in deeper water (>2,000 m) have higher S contents (0.09–0.12 wt.%;

Clague and Calvert 2009) indicative of eruption at depths >1,000 mbsl (Moore and Fabbi 1971; Davis et al. 2003). Lower S content glasses (0.01–0.03 wt.%), which are indicative of subaerial eruption, were collected 15 km east of the summit cone just below the lowermost (~1,340 mbsl) carbonate terrace (Clague and Moore 1991; Clague and Calvert 2009; see Fig. 3). Some of these glasses are from a hyaloclastite outcrop overlying pillow basalts. Are they from Mahukona or the neighboring, younger volcano Kohala? Unfortunately, many Mahukona tholeiitic samples overlap in glass composition and in Pb, Sr, and Hf isotopic ratios with Kohala tholeiites (Fig. 9), so we cannot determine whether these hyaloclastites are from Mahukona.

Hawaiian plume heterogeneity: Kea-like compositions in Loa trend volcano

The heterogeneity of the Hawaiian plume has been extensively investigated using radiogenic isotopes in basalts to infer mantle source characteristics (e.g., Weis et al. 2011, and references therein). Pb isotope trends show that the plume has an overall bilateral geochemical symmetry following the Loa and Kea trends of Hawaiian volcanoes (Tatsumoto 1978; Abouchami et al. 2005). However, as more lavas are analyzed, it has become clear that the simple bilateral symmetry model has exceptions. For example, lavas from several Hawaiian volcanoes have sampled both Kea and Loa sources (e.g., Mauna Kea, Eisele et al. 2003; Kohala, Abouchami et al. 2005; Haleakalā, Ren et al. 2006; Kīlauea, Marske et al. 2007; West Moloka`i, Xu et al. 2007; Ko`olau, Tanaka et al., 2002; Kaua`i, Garcia et al. 2010). Mahukona tholeiitic lavas also display both Loa and Kea-like Pb isotopic ratios with the higher silica lavas having Kea-like Pb isotope ratios (Fig. 9). Huang et al. (2009) noted both Loa- and Kea-like Pb isotopes among Mahukona samples, with most of their tholeiitic samples plotting in the Kea field (Fig. 10), despite Mahukona's location within the Loa trend (Fig. 1). A mixed peridotite and pyroxenite source was advocated for the Kea-like and Loa-like samples, respectively (Huang et al. 2009). This is opposite to what might be predicted from the higher silica content of our Kea-like samples (e.g., Hauri 1996; Stolper et al. 2004).

In contrast to the dominantly Kea-like Pb isotope values of Mahukona tholeiites, the transitional basalts are exclusively Loa-like in their Pb isotope systematics (Fig. 10). The presence of both Loa and Kea-like Pb compositions during the shield stage of growth, and the switch to only Loa-like compositions during the post-shield stage is inconsistent with a simple bilaterally asymmetrical plume model. The combined Mahukona results indicate considerable heterogeneity in the melting region for this volcano and also that the Hawaiian plume has more complex geochemical structure than predicted by either the simple concentrically or

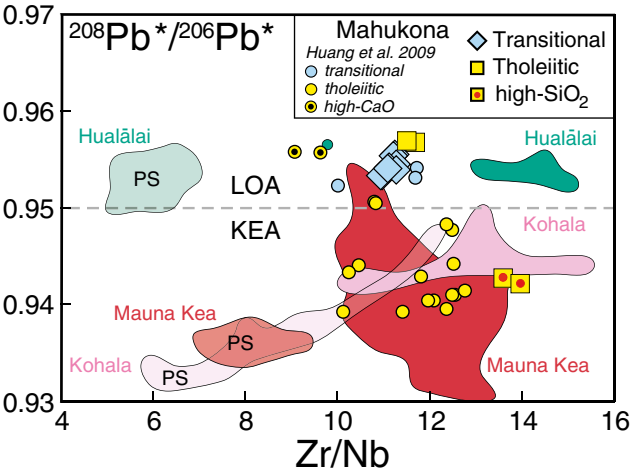

Fig. 10 Plot of radiogenic Pb isotopes vs. Zr/Nb for Mahukona basalts. The shield (tholeiitic) and post-shield lavas (alkalic, PS) from Hualālai and Kohala plot in appropriate Loa or Kea field for the location of their shield volcano (see Fig. 1), whereas Mahukona tholeiites and a few Mauna Kea tholeiites plot on both sides of the Loa-Kea line. Mahukona data from Tables 4 and 6 and Huang et al. (2009). Kohala, Mauna Kea, and Hualālai data from Hanano et al. (2010). Mauna Kea shield data from Eisele et al. (2003) and Rhodes and Vollinger (2004). $^{208}Pb^*/^{206}Pb^*$ is a measure of the radiogenic addition to $^{208}Pb/^{204}Pb$ and $^{206}Pb/^{204}Pb$ during Earth history and is calculated by subtracting the primordial (initial) isotope ratios from the measured values. $^{208}Pb^*/^{206}Pb^*$ reflects the ratio of Th/U integrated over the history of the Earth

bilaterally zoned models to explain the Loa-Kea trends (e.g., Hauri 1996; Kurz et al. 1996; Abouchami et al. 2005). These observations might result from sampling a wider portion of the Hawaiian plume during the hotter (higher degree of melting) shield stage than during the cooler (lower degree of melting) post-shield stage. This is consistent with the modeling of DePaolo and Stolper (1996), which showed shield volcanoes tap magma from a wide cross-sectional area of the plume. Alternatively, the compositional diversity may be related to the absence of a central magma reservoir where magmas would have been homogenized. This interpretation is supported by studies of melt inclusions in olivines that preserve more compositional diversity than observed in lavas (e.g., Maclennan 2008). Also, the small size of Mahukona probably reflects less mantle melting and preservation of source heterogeneities (e.g., Garcia et al. 2010).

The presence of relatively high $^{3}He/^{4}He$ (up to 20.8 Ra) in olivines and one glass from some transitional Mahukona samples is enigmatic. In Hawai`i, high $^{3}He/^{4}He$ values (≥20 Ra) are relatively rare and are only found in lavas from the pre-shield stage at Lō`ihi Seamount (up to 32 Ra; e.g., Kurz et al. 1983) and Kīlauea (up to 26.5 Ra; Hanyu et al. 2010) and some early stage tholeiites from Mauna Loa (20.0 Ra; Kurz et al. 1995) and Mauna Kea (up to 24.7 Ra; Kurz et al. 2004). The new and previous ^{40}Ar–^{39}Ar ages for Mahukona transitional lavas (~480 to 325 ka; Table 1; Clague and Calvert 2009)) indicate

Table 6 Pb, Hf, Sr, Nd, and He isotopic compositions of Mahukona basalts

Sample	$^{208}Pb/^{204}Pb$	2σ	$^{207}Pb/^{204}Pb$	2σ	$^{206}Pb/^{204}Pb$	2σ	$^{176}Hf/^{177}Hf$	2σ	$^{87}Sr/^{86}Sr$	2σ	$^{143}Nd/^{144}Nd$	2σ	$^{3}He/^{4}He$	1σ
159-1	37.9719	47	15.4670	17	18.1879	19	0.283063	7	0.703769	7	0.512907	6	11.5	0.1
159-4	38.1066	20	15.4776	8	18.3412	8	0.283089	4	0.703689	8	0.512929	7	18.1	0.3
159-6	38.0952	22	15.4703	7	18.3488	7	0.283095	4	0.703699	9	0.512945	6	nd	nd
160-1	38.1232	22	15.4771	7	18.3661	8	0.283089	4	0.703696	6	0.512938	6	nd	nd
160-2	38.0636	18	15.4719	7	18.3076	8	0.283092	5	0.703682	9	0.512932	6	15.8	0.2
160-5	38.0494	16	15.4697	6	18.2944	6	0.283084	4	0.703689	7	0.512925	6	19.5	0.3
160-6	38.0495	16	15.4699	6	18.2936	6	0.283088	5	0.703687	7	0.512939	6	18.4	0.3
											olivine furnace		13.5	3.0
161-1	37.9514	23	15.4669	8	18.2983	9	0.283125	6	0.703586	9	0.513001	6	19.1	0.3
	37.9512	17	15.4665	6	18.2980	7	0.283125	4	0.703581	7	0.513013	7	nd	nd
161-2	37.9395	29	15.4611	10	18.2913	11	0.283126	8	0.703569	7	0.512991	7	13.1	0.1
161-4	37.9750	25	15.4680	11	18.1901	11	0.283067	6	0.703776	9	0.512911	6	13.7	0.1
MA-12	38.0624	21	15.4683	7	18.3147	8	0.283086	5	0.703686	7	0.512942	6	20.8	0.9
							0.283090	4						
MA-32	38.1446	19	15.4820	7	18.3795	8	0.283089	4	0.703674	7	0.512929	6	20.2	0.1

Pb isotopic ratios were normalized to the NBS 981 triple spike values of Galer and Abouchami (1998) using the standard bracketing method; Hf data were normalized to JMC 475 ($^{176}Hf/^{177}Hf$=0.282160 (Vervoort and Blichert-Toft, 1999)). Sr data were normalized to SRM 987 $^{87}Sr/^{86}Sr$=0.710248; Nd data were normalized to La Jolla $^{143}Nd/^{144}Nd$=0.511858 (Weis et al. 2006). The 2σ error is the absolute error value of an individual sample analysis (internal error) and applies to the last decimal place(s). $^{3}He/^{4}He$ ratios are reported relative to air (R/R_{air}) where air=1.384×10^{-6}. All helium measurements were made at WHOI by crushing olivine in vacuo (except MA-32 which was on glass). He isotope data for MA samples from Garcia et al. (1990)

these lavas are younger than the tholeiites and not from the pre-shield stage. Thus, Mahukona is the only known example of late-stage Hawaiian volcanism with high $^{3}He/^{4}He$ and is an important exception to the generally observed temporal evolution and to models for the zoning of the Hawaiian plume (e.g., Kurz et al. 2004). The Pb and Sr isotope ratios of the transitional Mahukona lavas with high He isotope ratios are also similar to the high He isotope ratios in transitional and alkalic samples from Lō`ihi (Fig. 11). Perhaps during the post-shield stage, Mahukona tapped a source component similar to that of Lō`ihi. High He isotope ratios have also been observed in the post-shield Marquesas alkalic lavas, where it was related to sampling the "true" composition of the mantle source (Castillo et al. 2007). However, the Hawaiian plume is thought to be strongly heterogeneous with many components (e.g., Staudigel et al. 1984; Kurz et al. 2004; Weis et al. 2011). The Mahukona He isotope results suggest the Lō`ihi component in the Hawaiian plume is not restricted to the pre-shield stage and can also appear in the shield (Kaua`i, Mukhopadhyay et al. 2003; Mauna Kea, Kurz et al., 2004; and Mahukona) and post-shield stages (Mahukona).

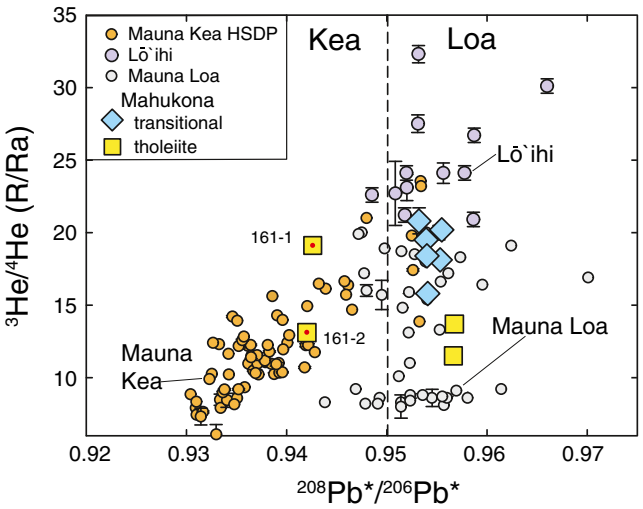

Fig. 11 Plot of $^{208}Pb^{*}/^{206}Pb^{*}$ against $^{3}He/^{4}He$ for the Mahukona samples. Also shown for comparison are data from nearby Mauna Loa (Kurz and Kammer 1991; Kurz et al. 1995), Mauna Kea (Kurz et al. 2004; Blichert-Toft et al. 2003), and Lō`ihi volcanoes (Kurz et al. 1983; Staudigel et al. 1984). Note that He-Pb compositions for Mahukona transitional basalt overlap with Lō`ihi samples (Garcia et al. 1990), although Mahukona tholeiites fall in both Kea and Loa fields

Summary

Three submersible dives, two dredge hauls, and a geophysics survey of Mahukona Volcano have resulted in new lava samples, new detailed bathymetric, sidescan sonar, and gravity maps. These maps, modeling of the gravity data and petrologic and geochemical analyses of the lavas show:

1. Cones on Mahukona are widespread (rather than being concentrated along rift zones). No residual gravity anomaly was found centered over the bathymetric high.

Both features are atypical for Hawaiian shield volcanoes and suggest the volcano did not have a long-lived central magma reservoir.

2. Mahukona is one of the smallest Hawaiian volcanoes (~6,000 km^3) based on modeling the new bathymetric and gravity data, which is consistent with its small residual gravity high (maximum of 20–25 mGal).
3. The reconstructed subsidence history (900 to at least 1,700 m over 350–650 kyrs) based on the new ^{40}Ar–^{39}Ar ages), moderate vesicularity of the lavas, and low-to-moderate S contents of glasses suggest Mahukona Volcano probably did not breach sea level but came within a few hundred meters of it.
4. The new ^{40}Ar–^{39}Ar ages document the periods of late shield tholeiitic (~650 ka) and post-shield transitional (~480–350 ka) volcanism on Mahukona. The volcano probably ceased volcanism at ~325 ka (averaged age for summit cone from new and previous ages), whereas neighboring Kohala Volcano continued erupting evolved alkalic lavas from 250 to 60 ka. Evolved alkalic lavas have not been sampled on Mahukona. Thus, Mahukona Volcano went extinct prematurely.
5. Tholeiitic and transitional lavas are common on Mahukona, but more alkaline rocks have not been recovered. The tholeiitic lavas include higher SiO_2 lavas, which are distinct in trace elements and isotopes. The higher SiO_2 lavas in our study and many of the previously studied Mahukona tholeiites overlap in Pb isotope ratios with lavas from Kohala, a Kea trend volcano. However, five tholeiitic lavas and all of the transitional lavas have Loa trend chemical affinities, consistent with the location of Mahukona in the Loa trend of Hawaiian volcanoes. Thus, Mahukona had a mixed source with both Loa- and Kea-like components.
6. Some Mahukona transitional lavas have high $^3He/^4He$ ratios (19–20 Ra) unlike any other Hawaiian post-shield lava. The Hawaiian plume is thought to be strongly heterogeneous with many components including the Lō`ihi component, which was the probable source for the higher He isotope ratios during the tholeiitic and post-shield volcanism stages at Mahukona.
7. The diversity of Mahukona lava chemistry, both in elemental abundance and in isotopic ratios, may be related to the relatively small size of Mahukona (less extensive melting) and the absence of a central magma reservoir where magmas would have been homogenized.

Acknowledgments We thank Terry Kirby and the other members of the Pisces V team for the successful dives on Mahukona; the captain and crew of the R/V Kilo Moana, R/V Kila, and R/V Atlantis II for assistance with surveying and sampling Mahukona; John Huard for ^{40}Ar–^{39}Ar ages; Mike Vollinger for XRF analyses; Charles Knaack for ICP-MS analyses; Jane Barling and Bruno Kieffer for their help in acquiring the isotopic data at PCIGR; Joshua Curtice for assistance with helium measurements; and the reviewers (S. Huang, D. Clague, and an anonymous reviewer) and the editor, M. Clynne, of this paper for their constructive comments. This work was supported by NSF grant EAR05-10482 to MOG and GI, and a NSERC Discovery Grant to DW. Our 2009 expedition was funded by the State of Hawai`i, through SOEST as a student research cruise. This paper is SOEST Contrib. #8608.

References

Abouchami W, Hofmann AW, Galer SJG, Frey FA, Eisele J, Feigenson M (2005) Lead isotopes reveal bilateral asymmetry and vertical continuity in the Hawaiian mantle plume. Nature 434:851–856. doi:10.1038/nature03402

Batiza R, Vanko D (1983) Volcanic development of small oceanic central volcanoes on the flanks of the East Pacific Rise inferred from narrow beam echo-sounder surveys. Mar Geol 54:53–90

Blichert-Toft J, Frey FA, Albarède F (1999) Hf isotope evidence for pelagic sediments in the source of Hawaiian basalts. Science 285:879–882

Blichert-Toft J, Weis D, Maerschalk C, Agranier A, Albarède F (2003) Hawaiian hot spot dynamics as inferred from the Hf and Pb isotope evolution of Mauna Kea volcano. Geochem Geophys Geosyst 4:8704. doi:10.1029/2002GC00340

Bryce JG, DePaolo DJ, Lassiter JC (2005) Geochemical structure of the Hawaiian plume: Sr, Nd, and Os isotopes in the 2.8 km HSDP-2 section of Mauna Kea volcano. Geochem Geophys Geosyst 6: Q09G18. doi:10.1029/2004GC000809

Castillo P, Klein E, Bender J, Langmuir C, Shirey S, Batiza R, White W (2000) Petrology and Sr, Nd, and Pb isotope geochemistry of mid-ocean ridge basalt glasses from the 11 °45'N to 15 °00'N segment of the East Pacific Rise. Geochem Geophys Geosyst 1:1011. doi:10.1029/1999GC000024

Castillo PR, Scarsi P, Craig H (2007) He, Sr, Nd and Pb isotopic constraints on the origin of the Marquesas and other linear volcanic chains. Chem Geol 240:205–221

Clague DA, Calvert AT (2009) Postshield stage transitional volcanism on Mahukona volcano, Hawai`i. Bull Volcanol 71:533–539

Clague DA, Moore JG (1991) Geology and petrology of Mahukona volcano, Hawai`i. Bull Volcanol 53:159–172

Clague DA, Moore JG, Dixon JE, Friesen WB (1995) Petrology of submarine lavas from Kilauea's Puna Ridge, Hawai`i. J Petrol 36:299–349

Clague D, Moore JG, Reynolds JR (2000) Formation of flat-topped volcanic cones in Hawai'i. Bull Volcanol 62:214–233

Clouard V, Bonneville A, Barsczus HG (2000) Size and depth of ancient magma reservoirs under atolls and islands of French Polynesia using gravity data. J Geophys Res 105:8173–8191

Dana JD (1890) Characteristics of volcanoes. Dodd, Mead and Co, New York, p 399

Davis MG, Garcia MO, Wallace P (2003) Volatiles in glasses from Mauna Loa, Hawai`i: implications for magma degassing and contamination, and growth of Hawaiian volcanoes. Contrib Mineral Petrol 144:570–591

DePaolo DJ, Stolper EM (1996) Models of Hawaiian volcano growth and plume structure: implications of results from the Hawai`i Scientific Drilling Project. J Geophys Res 101:11,643–11,654

Eisele J, Abouchami W, Galer SJG, Hofmann AW (2003) The 320 kyr Pb isotopic evolution of Mauna Kea lavas recorded in the HSDP-2 drill core. Geochem Geophys Geosyst 4:8710. doi:10.1029/2002GC000339

Feigenson MD, Hofmann AW, Spera FJ (1983) Case studies on the origin of basalt: II, the transition from tholeiitic to alkalic volcanism on Kohala volcano, Hawai`i. Contrib Mineral Petrol 84:390–405

Flinders A, Ito G, Garcia MO (2010) Gravity anomalies of the Northern Hawaiian Islands: implications on the shield evolution of Kauai and Niihau. J Geophys Res 115:B08412. doi:10.1029/2009JB006877

Fornari D, Garcia MO, Tyce R, Gallo D (1988) Morphology and structure of Loihi Seamount based on SeaBeam sonar mapping. J Geophys Res 93:15,227–15,238

Frey FA, Wise W, Garcia MO, West H, Kwon ST (1990) Evolution of Mauna Kea Volcano, Hawai`i: Petrologic and geochemical constraints on postshield volcanism. J Geophys Res 95:1271–1300

Gaffney AM, Nelson BK, Blichert-Toft J (2005) Melting in the Hawaiian plume at 1–2 Ma as recorded at Maui Nui: the role of eclogite, peridotite and source mixing. Geochem Geophys Geosyst 6:Q10L11. doi:10.1019/2005GC000927

Galer SJG, Abouchami W (1998) Practical application of lead triple spiking for correction of instrumental mass discrimination. Mineral Mag 62A:491–492

Garcia MO (1996) Petrography, olivine and glass chemistry of lavas from the Hawai`i Scientific Drilling Project. J Geophys Res 101:11,701–11,713

Garcia MO, Kurz M, Muenow D (1990) Mahukona: a missing Hawaiian volcano. Geology 18:1111–1114

Garcia MO, Caplan-Auerbach J, De Carlo EH, Kurz MD, Becker N (2006) Geology, geochemistry and earthquake history of Loihi seamount, Hawai`i's youngest volcano. Chemie der Erde 66:81–108

Garcia MO, Ito G, Weis D et al (2008) Widespread secondary volcanism around the northern Hawaiian Islands. EOS Trans Am Geophy Un 89(52):542–543

Garcia MO, Swinnard L, Weis D, Greene AR, Tagami T, San H, Gandy CE (2010) Petrology, geochemistry and geochronology of Kaua`i lavas over 4.5 Ma: implications for the origin of rejuvenated volcanism and the evolution of the Hawaiian plume. J Petrol 51:1507–1540. doi:10.1093/petrology/egq027

Hanano D, Weis D, Scoates JS, Aciego S, DePaolo DJ (2010) Horizontal and vertical zoning of heterogeneities in the Hawaiian mantle plume from the geochemistry of consecutive post-shield volcano pairs: Kohala-Mahukona and Mauna Kea-Hualalai. Geochem Geophys Geosyst 11:Q01004. doi:10.1029/2009GC002782

Hanyu T, Kimura JI, Katakuse M, Calvert AT, Sisson TW, Nakai S (2010) Source materials for inception stage Hawaiian magmas: Pb-He isotope variations for early Kilauea. Geochem Geophys Geosyst 11:Q0AC01. doi:10.1029/2009GC002760

Hauri EH (1996) Major-element variability in the Hawaiian mantle plume. Nature 382:415–419

Hofmann AW (1988) Chemical differentiation of the Earth: the relationship between mantle, continental crust, and oceanic crust. Earth Planet Sci Lett 90:297–314

Holcomb RT (1987) Eruptive history and long-term behavior of Kilauea Volcano. US Geol Surv Prof Paper 1350:261–350

Holcomb RT, Nelson BK, Reiners PW, Sawyer N-L (2000) Overlapping volcanoes: the origin of Hilo Ridge, Hawai`i. Geology 28:547–550

Huang S, Frey FA, Blichert-Toft J, Fodor RV, Bauer GR, Xu G (2005) Enriched components in the Hawaiian plume: evidence from Kahoolawe volcano, Hawai`i. Geochem Geophys Geosyst 6:Q11006. doi:10.1029/2005GC001012

Huang S, Abouchami W, Blichert-Toft J, Clague DA, Cousens BL, Frey FA, Humayun M (2009) Ancient carbonate sedimentary signature in the Hawaiian plume: evidence from Mahukona volcano, Hawai`i. Geochem Geophys Geosyst 10:Q08002. doi:10.1029/2009GC002418

Kauahikaua J, Hildenbrand T, Webring M (2000) Deep magmatic structures of Hawaiian volcanoes, imaged by three-dimensional gravity models. Geology 28:883–886

Kinoshita WT, Krivoy HL, Mabey DR, MacDonald RR (1963) Gravity survey of the island of Hawai`i. US Geol Surv Prof Paper 475C: C114–116

Kurz MD, Kammer DP (1991) Isotopic evolution of Mauna Loa Volcano. Earth Planet Sci Lett 103:257–269

Kurz MD, Jenkins WJ, Hart S, Clague D (1983) Helium isotopic variations in Loihi Seamount and the island of Hawai`i. Earth Planet Sci Lett 66:388–406

Kurz MD, Kenna T, Kammer DP, Rhodes JM, Garcia MO (1995) Isotopic evolution of Mauna Loa volcano: a view from the submarine south west rift. In: Rhodes JM, Lockwood, JP, Mauna Loa Revealed. Am Geophys Un Mono 92:289–306

Kurz MD, Kenna TC, Lassiter JC, DePaolo DJ (1996) Helium isotopic evolution of Mauna Kea volcano: first results from the 1-km drill core. J Geophys Res 101:11781–11791

Kurz MD, Curtice J, Lott DE III, Solow A (2004) Rapid helium isotopic variability in Mauna Kea shield lavas from the Hawaiian Scientific Drilling Project. Geochem Geophys Geosyst 5:Q04G14. doi:10.1029/2002GC000439

Le Bas MJ, Le Maitre RW, Streckeisen A, Zanettin B (1986) A chemical classification of volcanic rocks based on the total alkalis-silica diagram. J Petrol 27:745–750

Lockwood JP, Lipman PW (1987) Holocene eruptive history of Mauna Loa Volcano. US Geol Surv Prof Pap 1350:509–535

Ludwig KR, Szabo BJ, Moore JG, Simmons KR (1991) Crustal subsidence rate off Hawai`i determined from $^{234}U/^{238}U$ ages of drowned coral reefs. Geology 19:171–174

Macdonald GA, Katsura T (1964) Chemical composition of Hawaiian lavas. J Petrol 5:82–133

Macdonald GA, Abbott AT, Peterson FL (1983) Volcanoes in the sea. Univ Hawai`i Press, Honolulu, 517 p

Maclennan J (2008) Lead isotope variability in olivine-hosted melt inclusions from Iceland. Geochim Cosmochim Acta 72:4159–4179

Marske JP, Pietruszka AJ, Weis D, Garcia MO, Rhodes JM (2007) Rapid passage of a small-scale mantle heterogeneity through the melting regions of Kīlauea and Mauna Loa Volcanoes, Hawai'i. Earth Planet Sci Lett 259:34–50

Mattox TN, Mangan MT (1997) Littoral hydrovolcanic explosions: a case study of lava–seawater interaction at Kilauea volcano. J Volcanol Geotherm Res 75:1–17

McDonough WF, S-s S (1995) The composition of the Earth. Chem Geol 120:223–253

McDougall I, Swanson DA (1972) Potassium-argon ages of lavas from the Hawi and Pololu volcanic series, Kohala Volcano, Hawai`i. Geol Soc Am Bull 83:3731–3738

Moore JG (1987) Subsidence of the Hawaiian ridge. US Geol Surv Prof Paper 1350:85–100

Moore JG, Campbell JF (1987) Age of tilted reefs, Hawai`i. J Geophys Res 92:2641–2646

Moore JG, Fabbi BP (1971) An estimate of the juvenile sulfur content of basalt. Contrib Mineral Petrol 33:118–127

Moore RB, Clague DA, Rubin M, Bohrson WA (1987) Hualalai volcano: a preliminary summary of geologic, petrologic and geophysical data. US Geol Surv Prof Paper 1350:571–585

Moore JG, Normark WR, Szabo BJ (1990) Reef growth and volcanism on the submarine southwest rift zone of Mauna Loa Volcano. Bull Volcanol 52:375–380

Mukhopadhyay S, Lassiter JC, Farley KA, Bogue SW (2003) Geochemistry of Kaua`i shield-stage lavas: implications for the

chemical evolution of the Hawaiian plume. Geochem Geophys Geosyst 4:1009. doi:10.1029/2002GC000342

Niu Y, Collerson KD, Batiza R, Wendt JI, Regelous M (1999) Origin of enriched-type mid-ocean ridge basalt at ridges far from mantle plumes: the East Pacific Rise at 11°20'N. J Geophys Res 104 (B4):7067–7087

Pietruszka AP, Garcia MO (1999) A rapid fluctuation in the mantle source and melting history of Kilauea Volcano inferred from the geochemistry of its historical summit lavas (1790–1982). J Petrol 40:1321–1342

Prince RA, Forsyth DW (1984) A simple objective method for minimizing crossover errors in marine gravity data. Geophysics 49:1070–1083

Regelous M, Niu Y, Wendt JI, Batiza R, Greig A, Collerson K (1999) Variations in the geochemistry of magmatism on the East Pacific Rise at 10 °30'N since 800 ka. Earth Planet Sci Lett 168:45–63

Ren Z-Y, Shibata T, Yoshikawa M, Johnson K, Takahashi E (2006) Isotope compositions of submarine Hana Ridge lavas, Haleakala Volcano, Hawai`i: implications for source compositions, melting process and the structure of the Hawaiian plume. J Petrol 47:255–275

Rhodes JM, Vollinger MJ (2004) Composition of basaltic lavas sampled by phase-2 of the Hawai`i Scientific Drilling Project: geochemical stratigraphy and magma types. Geochem Geophys Geosyst 5:Q03G13. doi:10.1029/2002GC000434

Rhodes JM, Wenz KP, Neal CA, Sparks JW, Lockwood JP (1989) Geochemical evidence for invasion of Kilauea's plumbing system by Mauna Loa magma. Nature 337:257–260

Robinson JE, Eakins BW (2006) Calculated volumes of individual shield volcanoes at the young end of the Hawaiian Ridge. J Volcanol Geotherm Res 151:309–317. doi:10.1016/j.jvolgeores.2005.07.033

Rubin AM (1990) A comparison of rift-zone tectonics in Iceland and Hawai`i. Bull Volcanol 52:302–319

Sherrod DR, Sinton JM, Watkins SE, Brunt KM (2007) Geologic map of the State of Hawai`i. US Geol Surv Open-File Report 2007–1089

Spengler S, Garcia MO (1988) Geochemical evolution of Hawi Formation lavas, Kohala Volcano, Hawai`i: the hawaiite to trachyte transition. Contrib Mineral Petrol 99:90–104

Staudigel H, Zindler A, Hart SR, Leslie T, Chen C-Y, Clague DA (1984) The isotopic systematics of a juvenile intraplate volcano: Pb, Nd, and Sr isotope ratios of basalts from Loihi Seamount. Earth Planet Sci Lett 69:13–29

Stolper E, Sherman S, Garcia MO, Baker M, Seaman C (2004) Glass in the submarine section of the HSDP2 drill core, Hilo, Hawai`i. Geochem Geophys Geosyst 5:Q07G15. doi:10.1029/2003GC000553

Tanaka R, Nakamura E, Takahashi E (2002) Geochemical evolution of Koolau volcano, Hawai`i. In: Takahashi E, Lipman P, Garcia M, Naka J, Aramaki S, Hawaiian volcanoes deep underwater perspectives. Am Geophys Un Mono 128:311–332

Tatsumoto M (1978) Isotopic composition of lead in oceanic basalt and its implication to mantle evolution. Earth Planet Sci Lett 38:63–87

Vervoort JD, Blichert-Toft J (1999) Evolution of the depleted mantle: Hf isotope evidence from juvenile rocks through time. Geochim Cosmochim Acta 63:533–556

Walker GPL (1990) Geology and volcanology of the Hawaiian Islands. Pac Sci 44:315–347

Wanless VD, Garcia MO, Rhodes JM, Weis D, Norman M, Fornari DJ, Kurz M, Guillou H (2006) Submarine radial vents on Mauna Loa Volcano, Hawai`i. Geochem Geophys Geosyst 7:Q05001. doi:10.1029/2005GC001086

Weis D, Kieffer B, Maerschalk C, Barling J, de Jong J, Williams GA, Hanano D, Pretorius W, Mattielli N, Scoates JS, Goolaerts A, Friedman RM, Mahoney JB (2006) High-precision isotopic characterization of USGS reference materials by TIMS and MC-ICP-MS. Geochem Geophys Geosyst 7:Q08006. doi:10.1029/2006GC001283

Weis D, Garcia MO, Rhodes JM, Jellinek M, Scoates JS (2011) Role of the Pacific ultra-low velocity zone in generating bilateral asymmetry in the Hawaiian mantle plume. Nature Geoscience 4:831–838. doi:10.1038/NGEO1328

Wessel P, Smith WHF (1998) New, improved version of the Generic Mapping Tools released. EOS Trans Am Geophys Un 79(47):579

West H, Garcia MO, Frey F, Kennedy A (1988) Evolution of alkalic cap lavas, Mauna Kea Volcano, Hawai`i. Contrib Mineral Petrol 100:383–397

Wolfe EW, Wise SW, Dalrymple B (1997) The geology and petrology of Mauna Kea Volcano, Hawai`i—a study of postshield volcanism. US Geol Surv Prof Paper 1557:1–129

Wright TL (1971) Chemistry of Kilauea and Mauna Loa lava in space and time. US Geol Surv Prof Paper 735:1–40

Xu G, Frey FA, Clague DA, Abouchami W, Blichert-Toft J, Cousens B, Weisler M (2007) Geochemical characteristics of West Molokai shield- and postshield-stage lavas: constraints on Hawaiian plume models. Geochem Geophys Geosyst 8: Q08G21. doi:10.1029/2006GC001554

Yamasaki S, Kani T, Hanan BB, Tagami T (2009) Isotopic geochemistry of Hualalai shield stage tholeiitic basalts from submarine North Kona region, Hawai`i. J Volcanol Geotherm Res 185:223–230